AN ABSTRACT OF THE THESIS OF

JO ELLEN GRETZINGER KELLNER for the MASTER OF SCIENCE
(Name) (Degree)

GENERAL SCIENCE
in (RADIOLOGICAL PHYSICS) presented on September 2, 1971
(Major) (Date)

Title: SCATTERED RADIATION FROM BEDSIDE RADIOGRAPHIC EXAMINATIONS

Abstract approved: Redacted for Privacy
John P. Kelley

The purpose of this study was to investigate the distribution and magnitude of scattered radiation from a typical mobile radiographic examination as an aid in evaluating the potential health hazards of the scattered radiation. Also discussed are current radiation protection standards and recommendations for mobile radiography.

A Masonite phantom represented the patient as a scattering medium, and was exposed to the radiation from a typical mobile x-ray unit using a geometry corresponding to an abdominal examination. Measurements of tube housing leakage and scatter were made for the ranges of kilovoltages and field sizes, with data points taken in a horizontal plane around one side of the phantom.

The magnitude of the scatter exposure was determined, and from this it was concluded that scatter can represent a potential hazard to the patient in an adjoining bed and to the operator. It was also concluded that although scatter

exposures were not in violation of current exposure limits, they could present a long-range problem and that it would be wise to reexamine existing protection requirements with the intent of creating a safer radiation situation.

Scattered Radiation from Bedside Radiographic Examinations

by

JoEllen Gretzinger Kellner

A THESIS

submitted to

Oregon State University

in partial fulfillment of
the requirements for the
degree of

Master of Science

June 1972

APPROVED:

Redacted for Privacy

Associate Professor of Electrical Engineering
In Charge of Major

Redacted for Privacy

Head of Department of General Science

Redacted for Privacy

Dean of Graduate School

Date thesis is presented Sept. 2, 1971

Typed by JoEllen Gretzinger Kellner

TABLE OF CONTENTS

LIST OF FIGURES

Figure | Page

LIST OF TABLES

SCATTERED RADIATION FROM BEDSIDE RADIOGRAPHIC EXAMINATIONS

I. INTRODUCTION

After their discovery in 1895, x rays were rapidly applied in the medical profession. The penetrating quality of the radiation made the diagnosis of wounds and lesions accurate and safe. However, in the course of such use, it became apparent that the radiation could cause severe biological damage from unnecessary or uncontrolled exposures. Burns and cancerous lesions were attributed to radiation exposures in both physics and medicine (16).

As knowledge in the field of radiology grew, groups of scientists and physicians formed to study the effects of radiation exposure and to make recommendations for the safe use of x rays.

The basic criteria for the safe use of x-rays as a medical tool are (1) to limit the useful beam to the area of examination by the use of collimators, (2) to eliminate non-penetrating radiations from the useful beam by use of filtration, and (3) to provide adequate protective shielding for the patient and the operator (42).

As early as 1927, stray radiation had been recognized as a potential health hazard to the radiologist. Landauer (30), in a published discussion, promoted the practice of carrying dental films on the person, to record the level of exposure received from stray radiation. However, at the time, exposure was expressed in terms of the erythema dose, the amount of x-radiation required to cause a reddening of the skin, and no reliable physical standard had yet been developed. In 1928, the roentgen, the physical unit of x-ray exposure, was formally established by the International Commission on Radiological Units and Measurements (ICRU).

The requirements for the operation of a mobile x-ray unit do not specify the use of shielding for personnel other than the operator; they merely state that the operator should stand at a minimum distance of six feet, and that he should use a protective shield or a protective apron (44).

The purpose of this study was to determine the magnitude of the scatter exposure from a typical bedside examination, as an aid in evaluating exposure risks and current radiation protection standards.

II. SCATTERED RADIATION

Modes of Interaction

Scattered radiation occurs whenever ionizing radiation interacts with matter. Scatter is defined as the radiation resulting from some form of interaction of the incident photons with matter. The major forms of interactions are the Compton effect, the photoelectric effect, coherent scattering, and pair production.

Pair production can occur whenever a photon of energy exceeding 1.022 MeV (million electron volts) passes near a nucleus. The photon is transformed into an electron-positron pair, which will eventually annihilate, emitting two photons of exactly 0.511 MeV each. This mode of interaction is not relevant to diagnostic procedures because the energy at which this process can occur is well above energies used in diagnostic procedures.

Coherent scattering occurs only at low energies, as a result of resonant absorption and radiation, with no net energy loss. This process is useful in crystal diffraction studies, but has no relevance in diagnostic radiology, since less than 5% of total scatter is due to coherent processes (25).

The photoelectric effect also involves the absorption of a photon, but in this case an electron from the atom is ejected. Secondary radiation is emitted as electrons cascade into the gap left by the ejected electron, and is termed fluorescent radiation. This mode of interaction is important in determining scatter exposure from high-Z materials. (Lindell (32) states that fluorescence is predominant in materials of higher atomic number than iron (Z=26), whereas Compton scatter is most important in the low-Z materials. Therefore, he concludes that iron would be the material of choice in shielding.)

Compton scattering results in the emission of an electron plus a photon of energy less than the energy of the incident photon. The secondary photon is emitted at an angle proportional to the fraction of energy transferred to the ejected electron. The energy of the scattered photon can be calculated using the relation

$$E' \text{ (MeV)} = \frac{E \text{ (MeV)}}{1 + a(1 - \cos \phi)}$$

where E is the energy of the incident photon in MeV, E' is the energy of the scattered photon in MeV, ϕ is the angle of scattering, and $a = \frac{E \text{ (MeV)}}{0.511 \text{ (MeV)}}$.

Maximum energy transfer occurs at a photon scattering angle of 180° (backscatter). At high values of photon energy E , the probability of a Compton interaction approaches zero. The probability of Compton scattering is relatively independent of the atomic number of the material (25).

Spectral Distribution of Scattered Radiation

The energy distribution of scattered radiation is similar to the distribution of the primary beam. Cormack and Burke (10) evaluated the distribution of scatter and the spectrum of the incident beam and found that the maximum scatter rate occurred at right angles to the primary beam, and that, in general, the average scattered energy was lower than the average primary beam energy. Hettinger (22) studied backscatter from various materials and found that in all cases the mean energy of the scatter was lower than the primary energy. Wilsey *et al.* (53) had previously found that lateral (*i. e.* 90^{o}) scatter differed little in spectral characteristics from the incident beam, but that scatter in the forward direction had a higher effective energy.

III. MATERIALS AND METHODS

Experimental Apparatus

A General Electric Mobile 100-15 x-ray unit was used for this study. The unit has a maximum rated voltage of 100 kilovolts peak (kVp) with tube current selections of 10 and 15 milliamperes. A Videx Corporation Mascot collimator and localizing cone assembly was provided.

Measurements were taken using a Victoreen Model 555 Radocon with interchangeable probes. A 555-10LA low energy probe was used to determine the beam quality at the specified voltages. This probe has an energy response near 1.00 in the range of 6 to 35 keV effective (50), and was used to determine the true effective beam energies at the voltages used. Leakage and scatter values were obtained using the 555-0.1DA diagnostic range probe, with an energy range of 20 to 250 keV effective. The energy response of this probe was ± 10% over the effective energy range of the useful beam from the x-ray unit. (50)

Figures 1 and 2 illustrate the experimental setup and geometry.

The phantom used was constructed of quarter-inch thick sheets of tempered Masonite, cut to represent a typical torso cross-section of dimensions 20 cm. by 30 cm. The length of the phantom was 72 cm. The Masonite sheets were

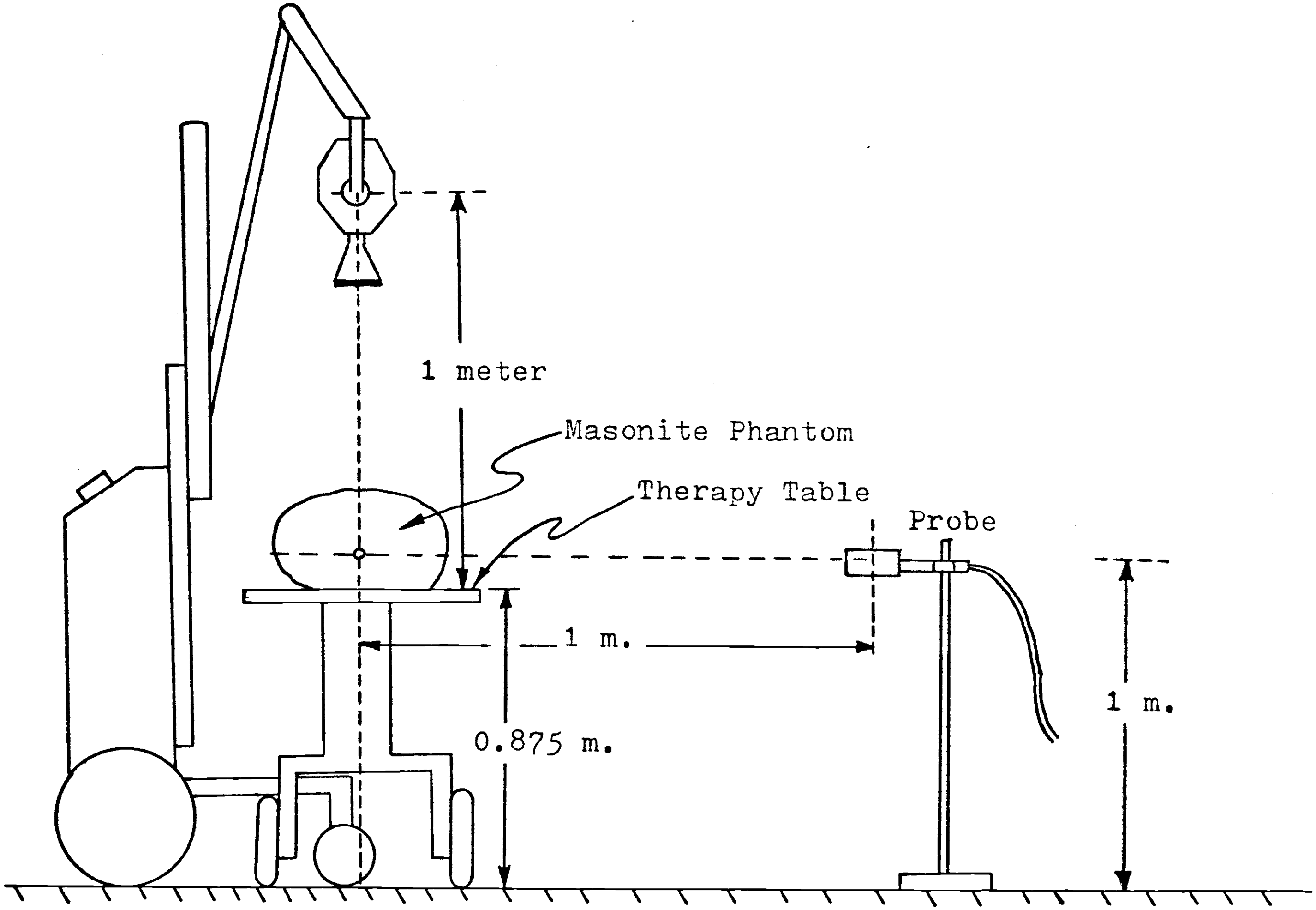

Figure 1. Experimental Apparatus and Measurement Geometry. Side View.

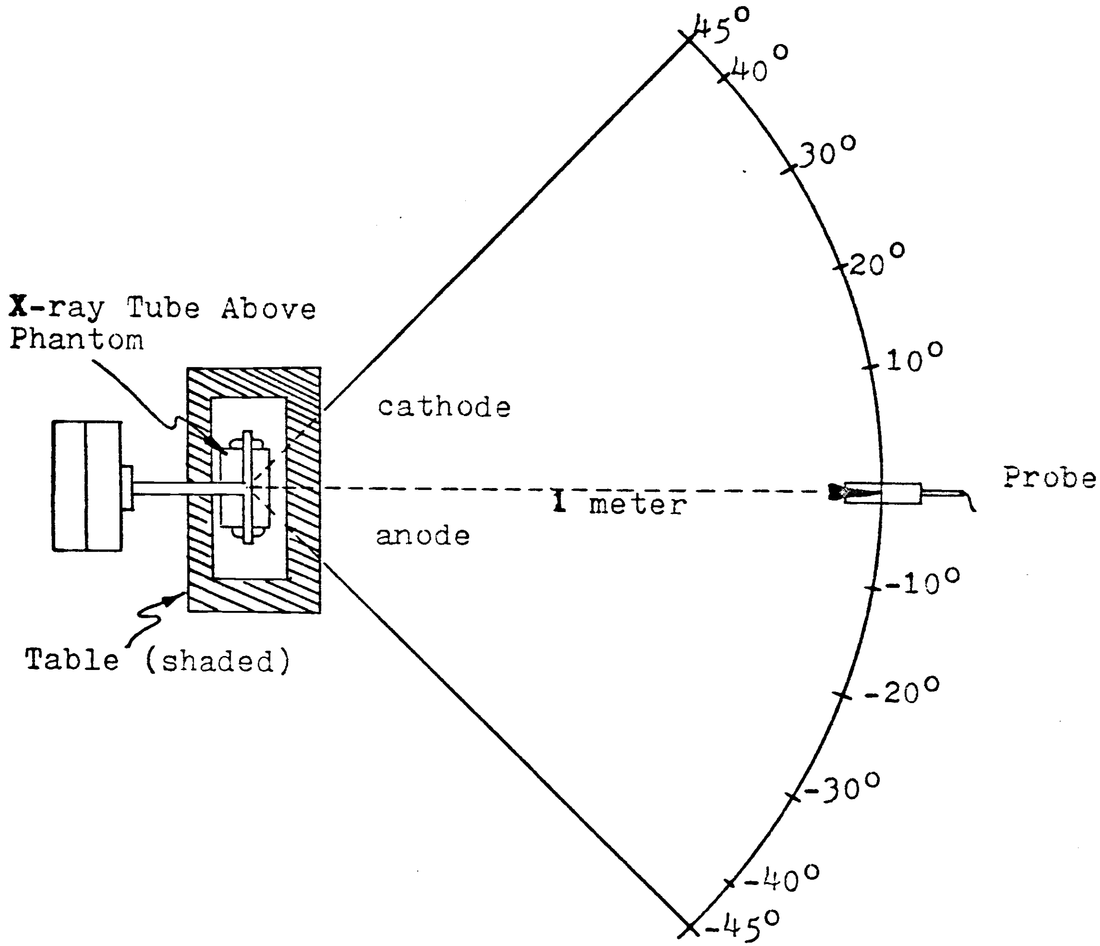

Figure 2. Experimental Apparatus and Geometry. Top View.

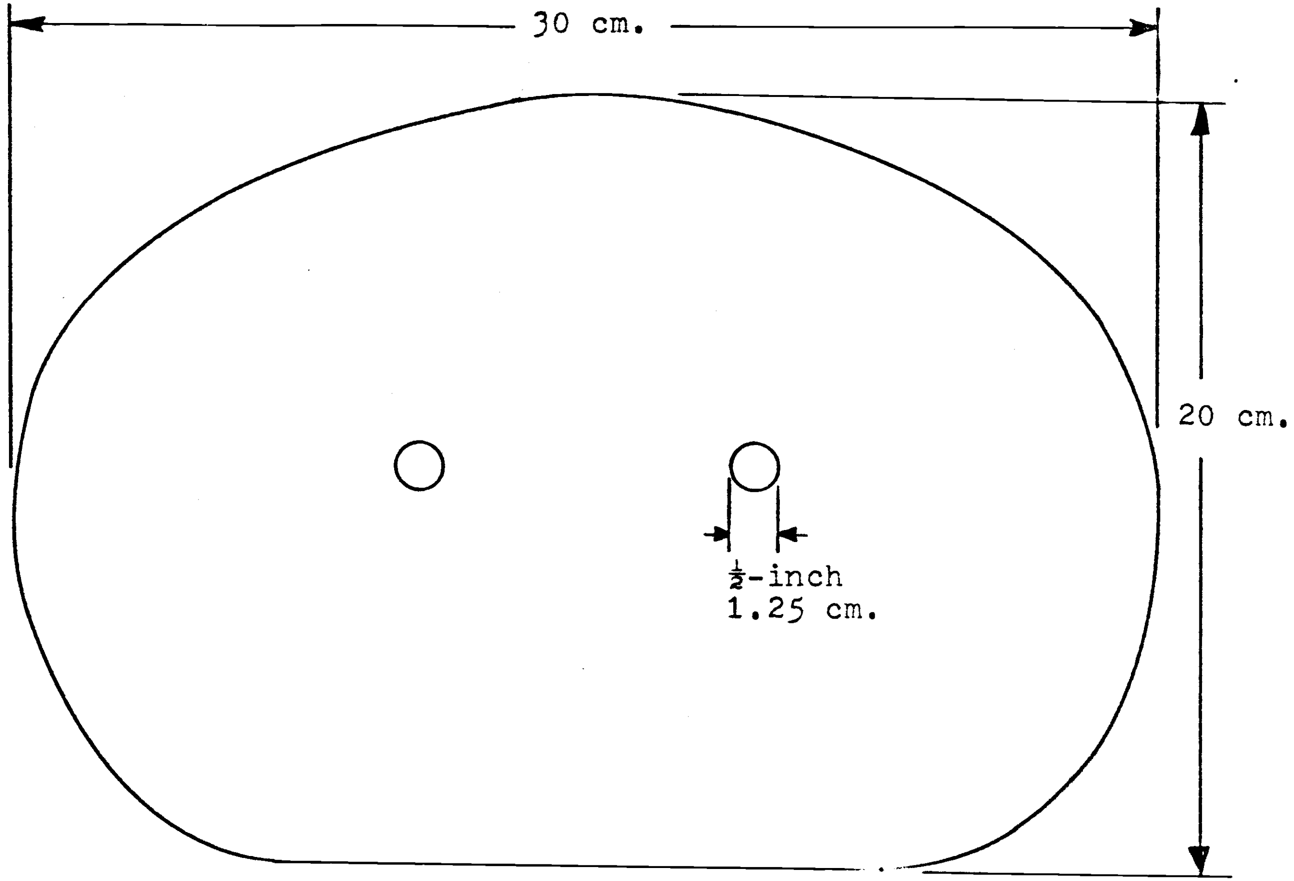

Figure 3. Cross-section of Masonite Phantom.

held together by two ½-inch diameter dowel rods down the long axis of the phantom. Masonite was chosen because of its similarity to tissue for radiation work, and also for its ready availability and low cost. Masonite has been used as a scattering medium in similar studies. Refer to Figure 3 for a diagram of the phantom cross-section.

A wood-topped therapy table supported the phantom at the height of the average hospital bed, 0.875 m. (28).

The Mascot collimator contained beam-defining blades controlled by a single lever. This system was determined to be unacceptable since commonly used rectangular fields could not be obtained. In order to cover the entire film the radiation field was larger than necessary. Lead diaphragms were cut to yield the desired field sizes at the film when they were inserted in the collimator at the position of the blades. The desired diaphragm sizes were obtained by using the similar triangles method:

$$\frac{\text{diaphragm width}}{\text{field width}} = \frac{11.8 \text{ cm.}}{100 \text{ cm.}}$$

where the distance from the focal spot to the position of the diaphragm was measured to be 11.8 cm. The calculated diaphragm sizes were:

field width (inches)	diaphragm width (inches)
8 x 10	0.924 x 1.155
10 x 12	1.155 x 1.386
14 x 17	1.617 x 1.964

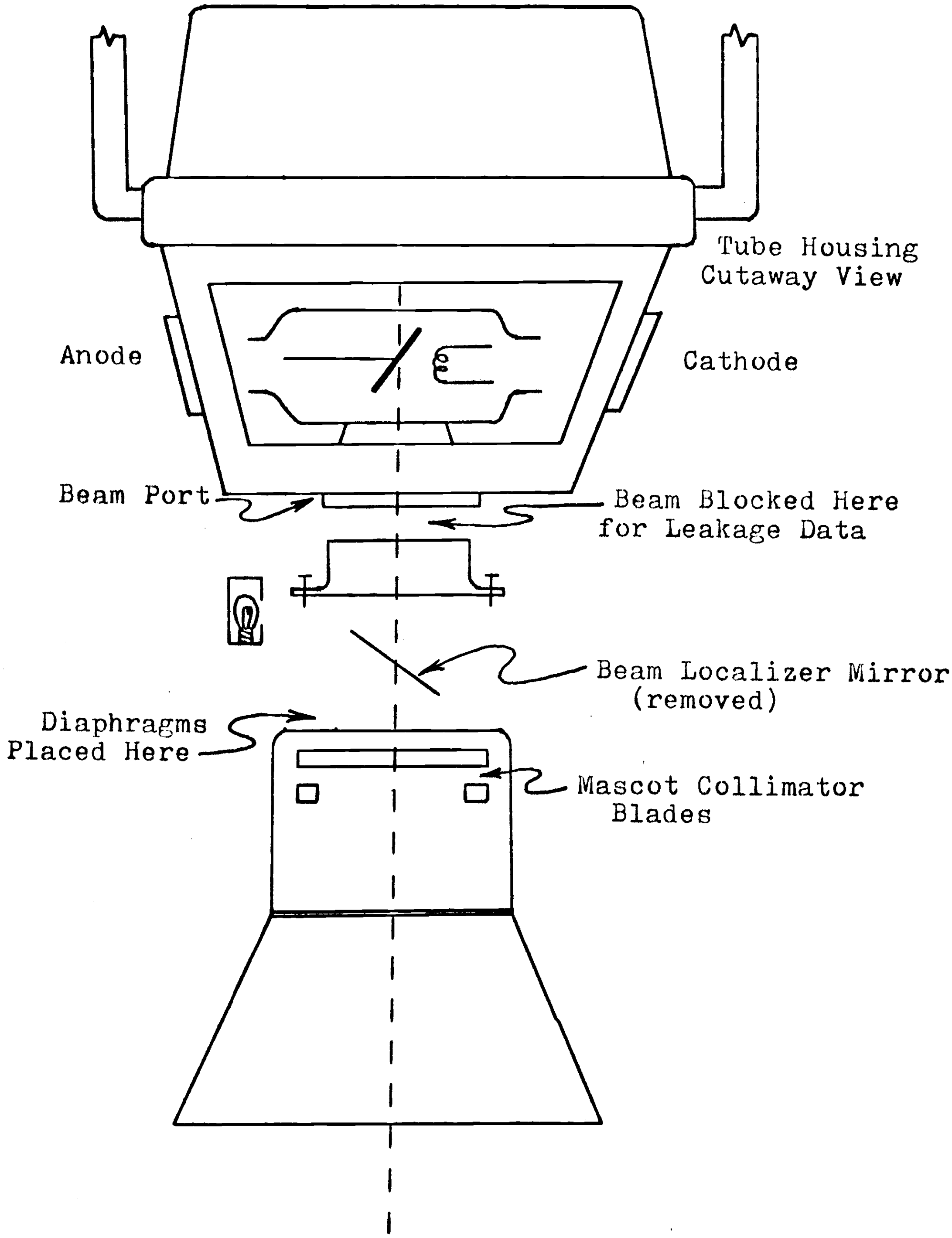

Figure 4. General Electric Mobile 100-15 Tube Housing with Modified Videx Corporation Mascot Collimator Assembly.

A field localization mirror was removed from the collimator assembly to reduce the inherent filtration of the unit to 2.5 mm. aluminum equivalent at 100 kVp, the minimum value set by the National Council on Radiation Protection and Measurements (NCRP) (40) and the Oregon State Board of Health (44).

Equipment Calibration

Beam quality and useful beam exposure rates were determined for the voltages used in this study. Inherent filtration and homogeneity coefficients were calculated. These results are summarized in Table 14.

Time response curves were determined for the rate scales of the Victoreen 555. Krc, the time response correction factor, corrects for the time constant of the instrument. The correction factors used in this study are listed in Table 15.

Energy response also affects the measured value of exposure. Ionization chamber response varies with the energy of the incident radiation. Therefore, it is necessary to know the energy response correction factors for each individually calibrated probe. Figure 21 is the correction curve plotted from data supplied by the Victoreen Company. Table 16 lists the energy response correction factors, Kr.

All unsealed ionization chambers of this type must also be corrected for variations in the ambient temperature and pressure. The probes are calibrated by the manufacturer at 22^{o} Celsius and 760 mm. mercury. Ktp, the temperature-pressure correction factor, can be calculated from the relation

$$Ktp = \left(\frac{273^{o} + T\ (^{o}C)}{295^{o}}\right)\left(\frac{760\ \text{mm.}}{P\ (\text{mm. Hg})}\right)$$

Experimental Procedure

The parameters of interest used in this study were: a fixed focus-film distance of one meter, a constant exposure of 50 milliampere-seconds (mAs), and field sizes of 8 x 10 inches, 10 x 12 inches, and 14 x 17 inches at the film. The x-ray field was centered on the phantom. Voltage was varied from 40 to 100 kVp in 20 kVp steps. The scatter exposure values were measured at a distance of one meter from the center of the phantom, in a horizontal plane about the phantom. The center of this horizontal field was arbitrarily designated 0^{o} and those angles to the anode side of the tube were indicated by a negative sign.

Tube housing leakage measurements were made for each angle with the beam blocked at the beam port by a thickness of lead exceeding the twentieth-value-layer.[1] The apparatus

[1] The twentieth-value-layer is the thickness of absorber (filter) required to reduce the exposure to .05 of the initial value.

was arranged in the exact geometry to be used in the determination of scatter. Many measurements were taken to insure statistical validity.

Scatter measurements were determined for each voltage and field size combination through the horizontal angle. Again, repetitive measurements were taken for validity. After the first complete set of data were taken, the entire setup was dismantled and then reassembled in the same geometry for more data. This was done to check the reliability of the technique used in this study. This method of taking data resulted in a maximum deviation of 38% (for one data point), with 93% of the data within 20% of the mean, 62% within 10%, and 36% within a 5% deviation.

IV. EXPERIMENTAL RESULTS

The measured values of leakage and scatter exposure were corrected independently for temperature and pressure, time response, and energy response, since these values varied within the same group of data points. The corrected exposure values were averaged and the net scatter exposure obtained by subtracting the corrected leakage exposure from the total exposure. All values are presented in units of milliroentgens per milliampere-second (mR/mAs).[2] The ratio of net scatter to incident useful beam was also calculated for each voltage and field size.

Figures 5 through 18 show the distribution of scattered radiation as a function of kilovoltage and of field size. The distributions are represented in both mR/mAs and percent of useful beam, at one meter. Appendix A contains the data in tabular form.

These graphs were drawn on polar logarithmic paper in order to best present the wide range of values. The data would be difficult to present and awkward to interpret in linear form.

---

[2]The roentgen is the unit of exposure for x- and gamma-radiation, and is defined as the amount of radiation required to produce 2.58×10^{-4} coulombs of charge per kilogram of dry air at standard temperature and pressure. (40)

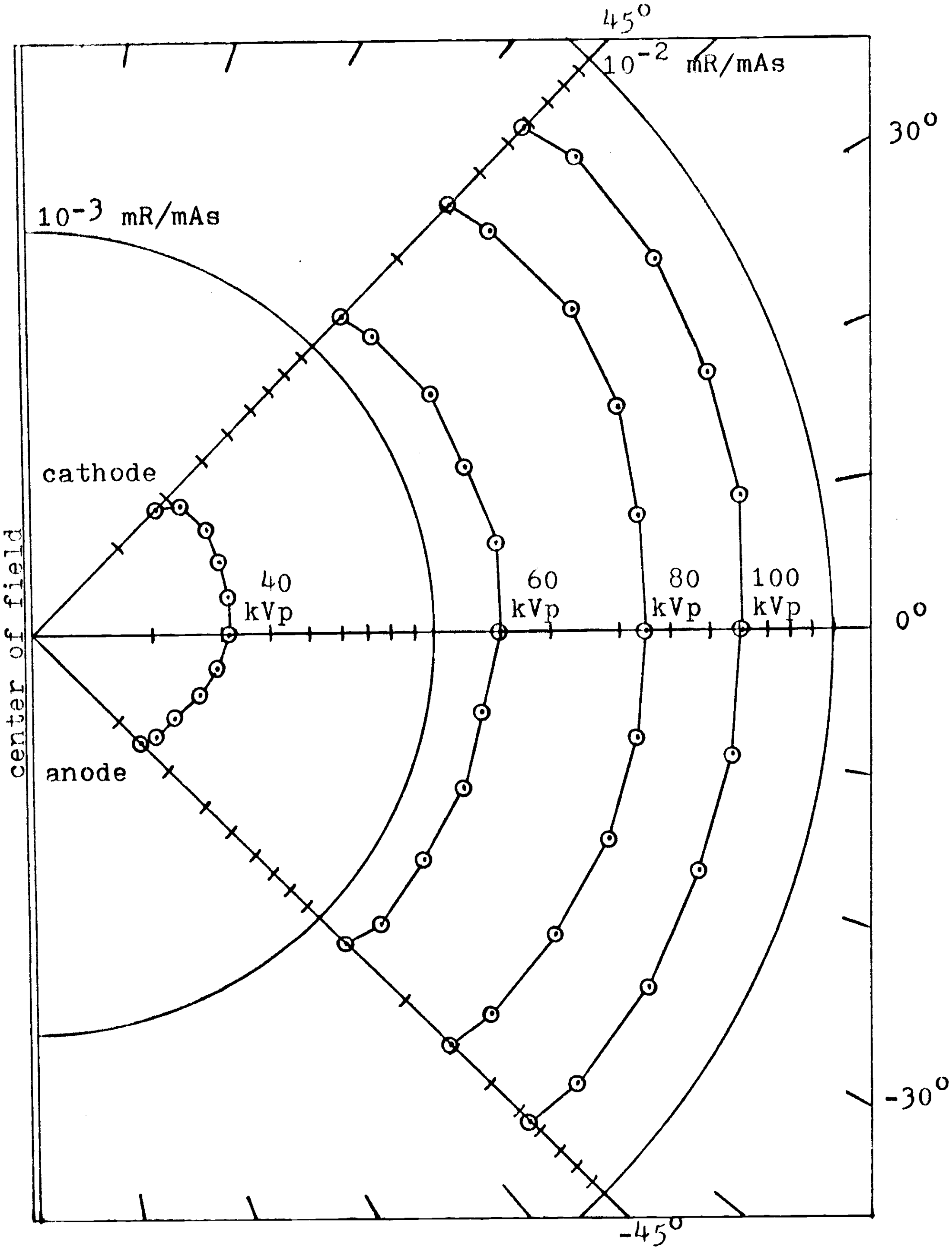

Figure 5. 90° Scatter Distribution from an 8 x 10-inch Field as a Function of Kilovoltage. Expressed in mR/mAs at One Meter.

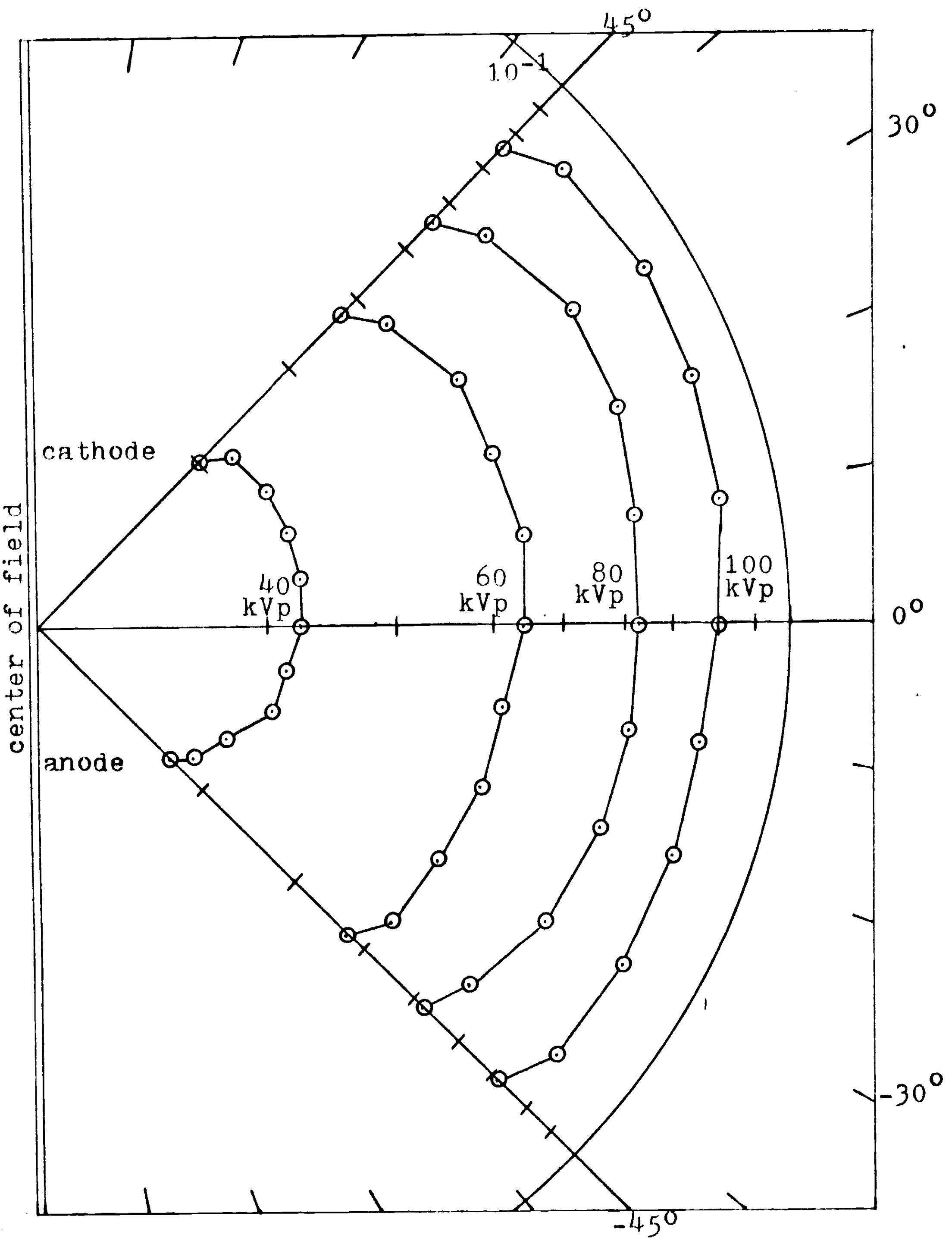

Figure 6. 90° Scatter Distribution from an 8 x 10-inch Field as a Function of Kilovoltage. Expressed in Percentage of Useful Beam at One Meter.

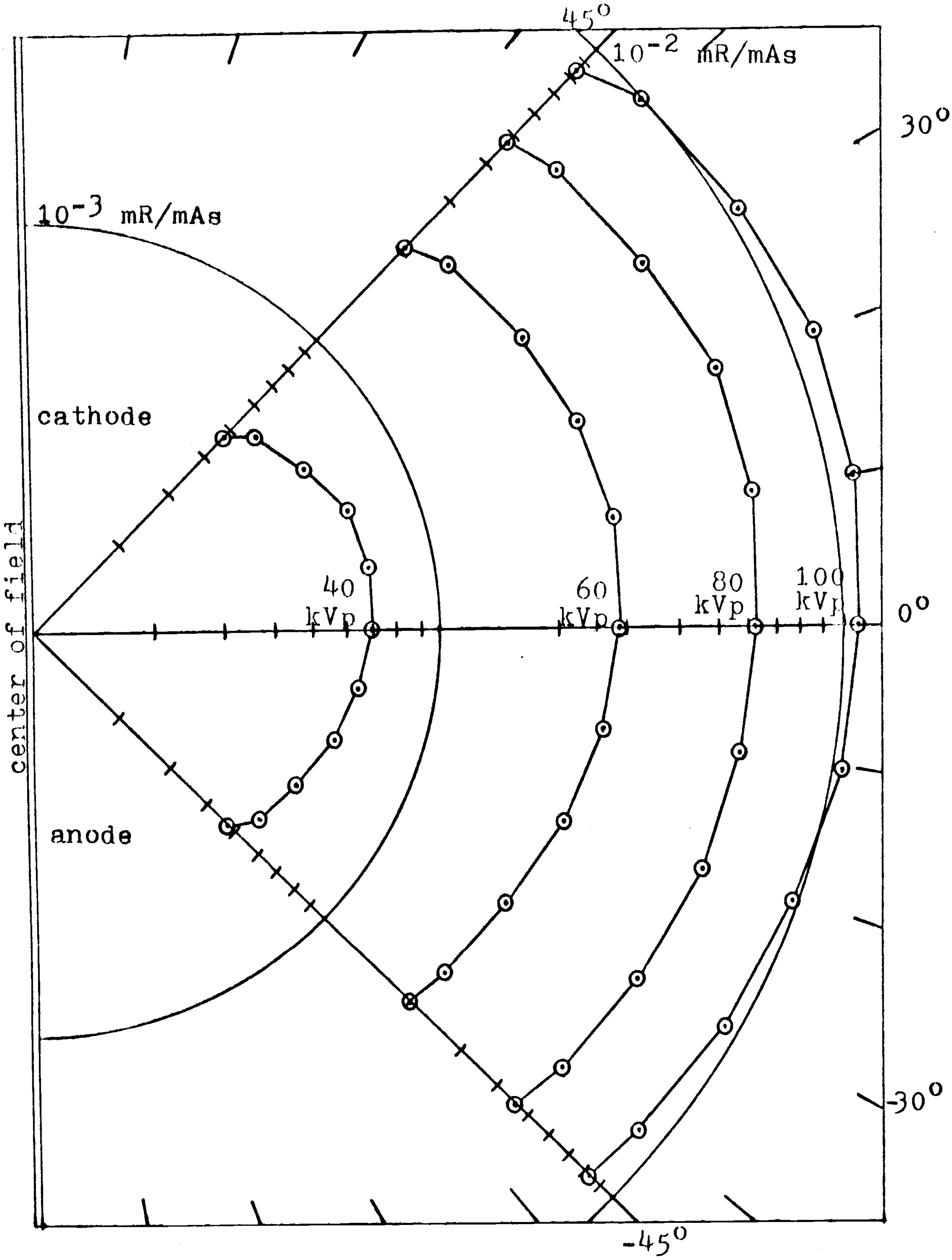

Figure 7. 90° Scatter Distribution from a 10 x 12-inch Field as a Function of Kilovoltage. Expressed in mR/mAs at One Meter.

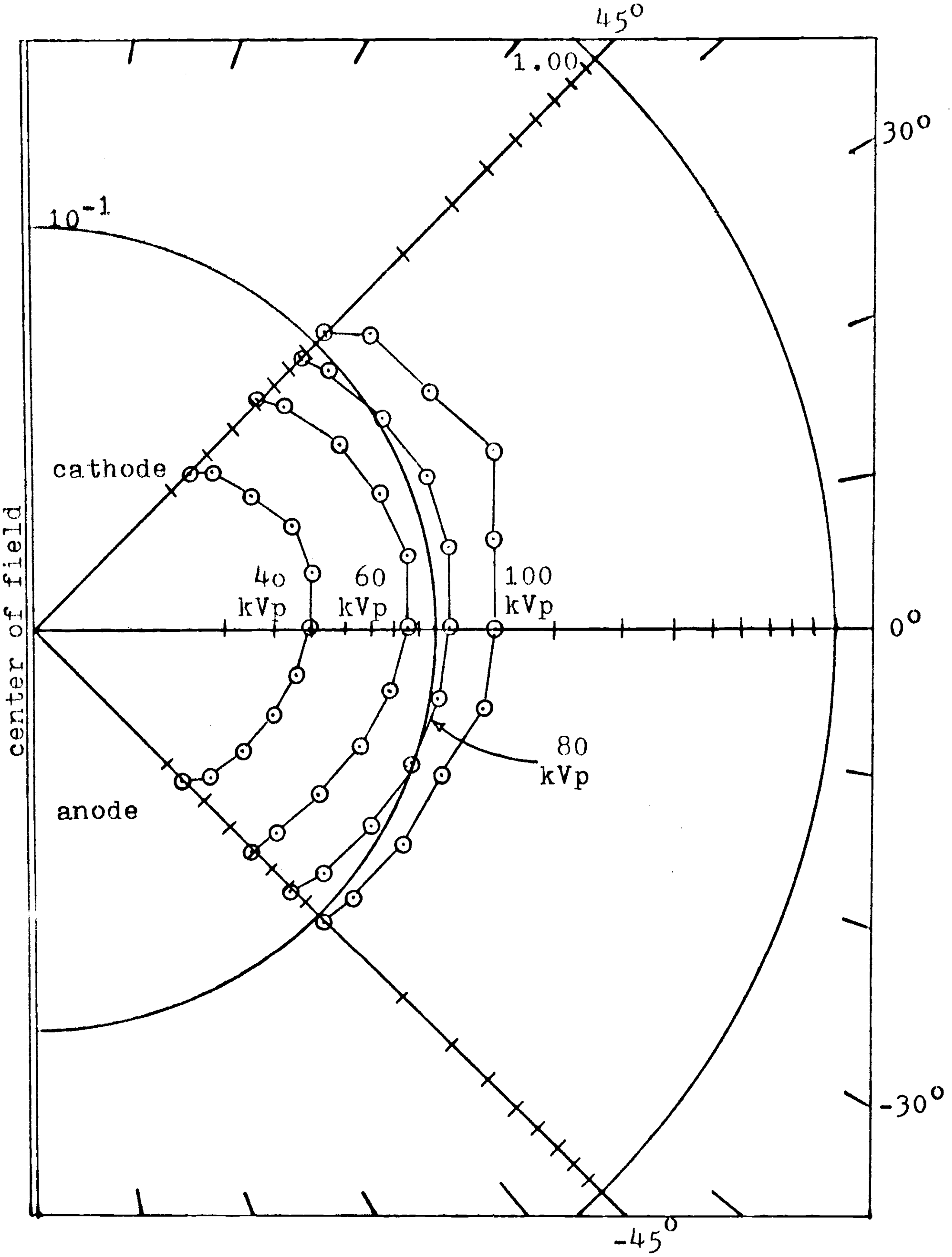

Figure 8. 90° Scatter Distribution from a 10 x 12-inch Field as a Function of Kilovoltage. Expressed in Percentage of Useful Beam at One Meter.

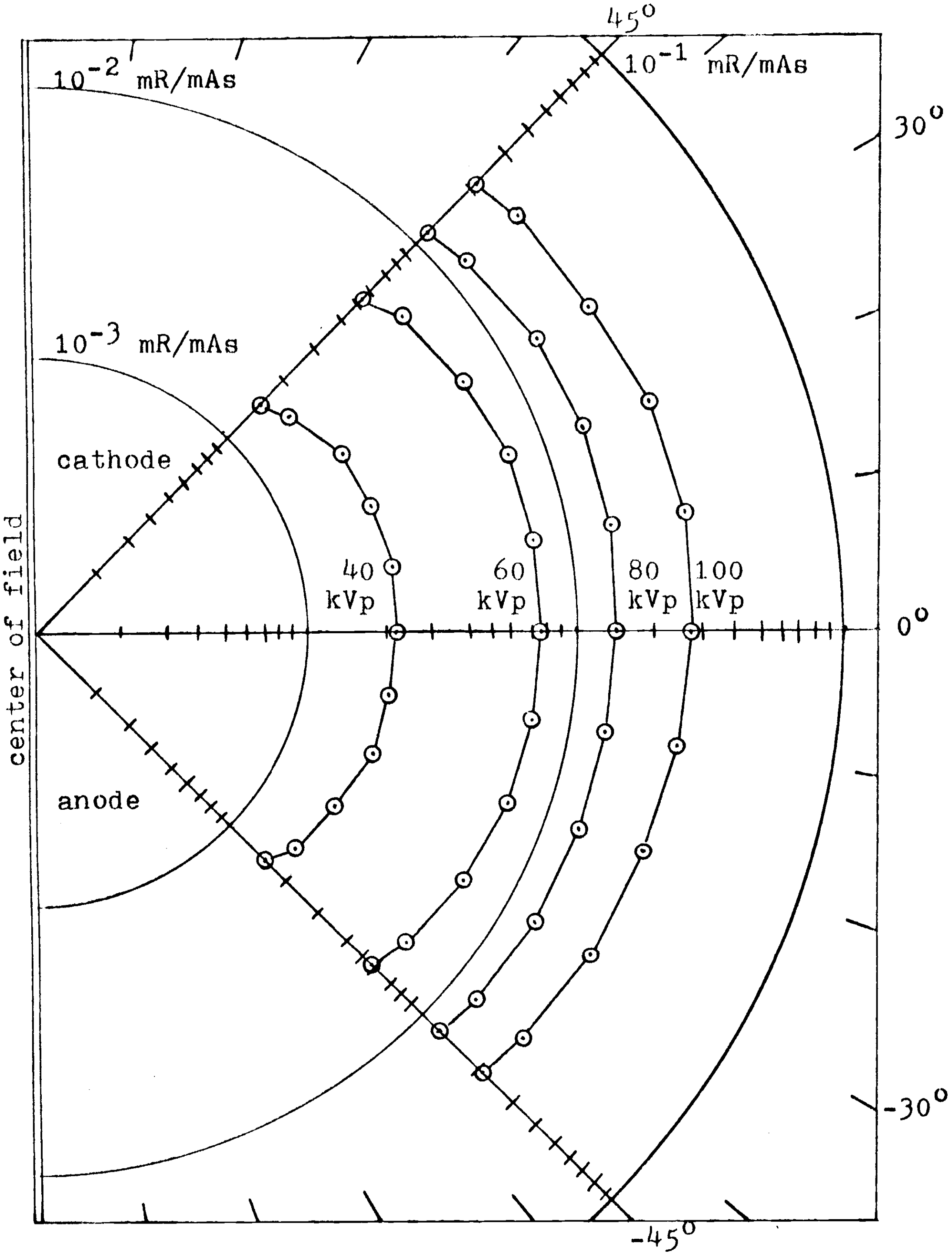

Figure 9. 90° Scatter Distribution from a 14 x 17-inch Field as a Function of Kilovoltage. Expressed in mR/mAs at One Meter.

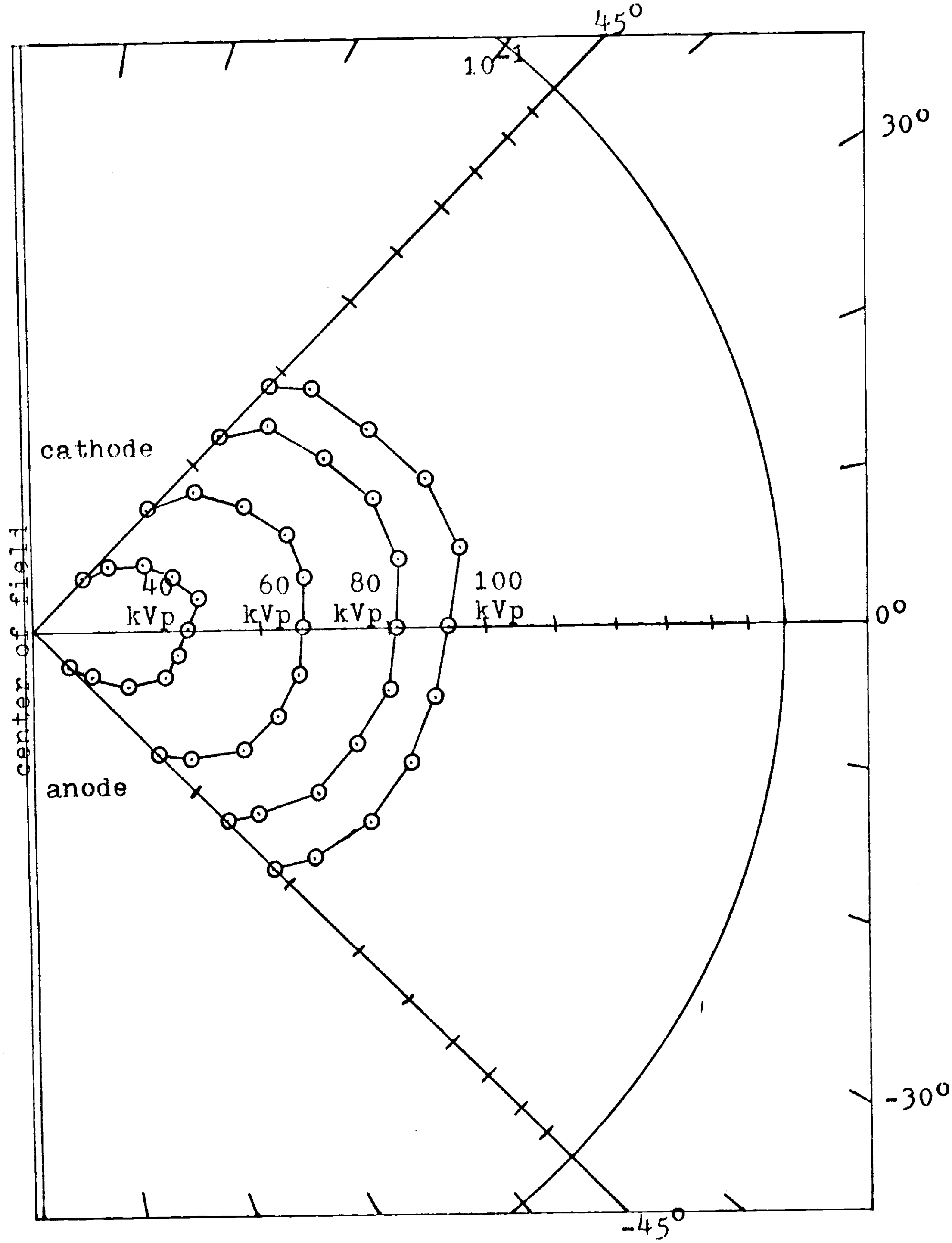

Figure 10. 90° Scatter Distribution from a 14 x 17-inch Field as a Function of Kilovoltage. Expressed in Percentage of Useful Beam at One Meter.

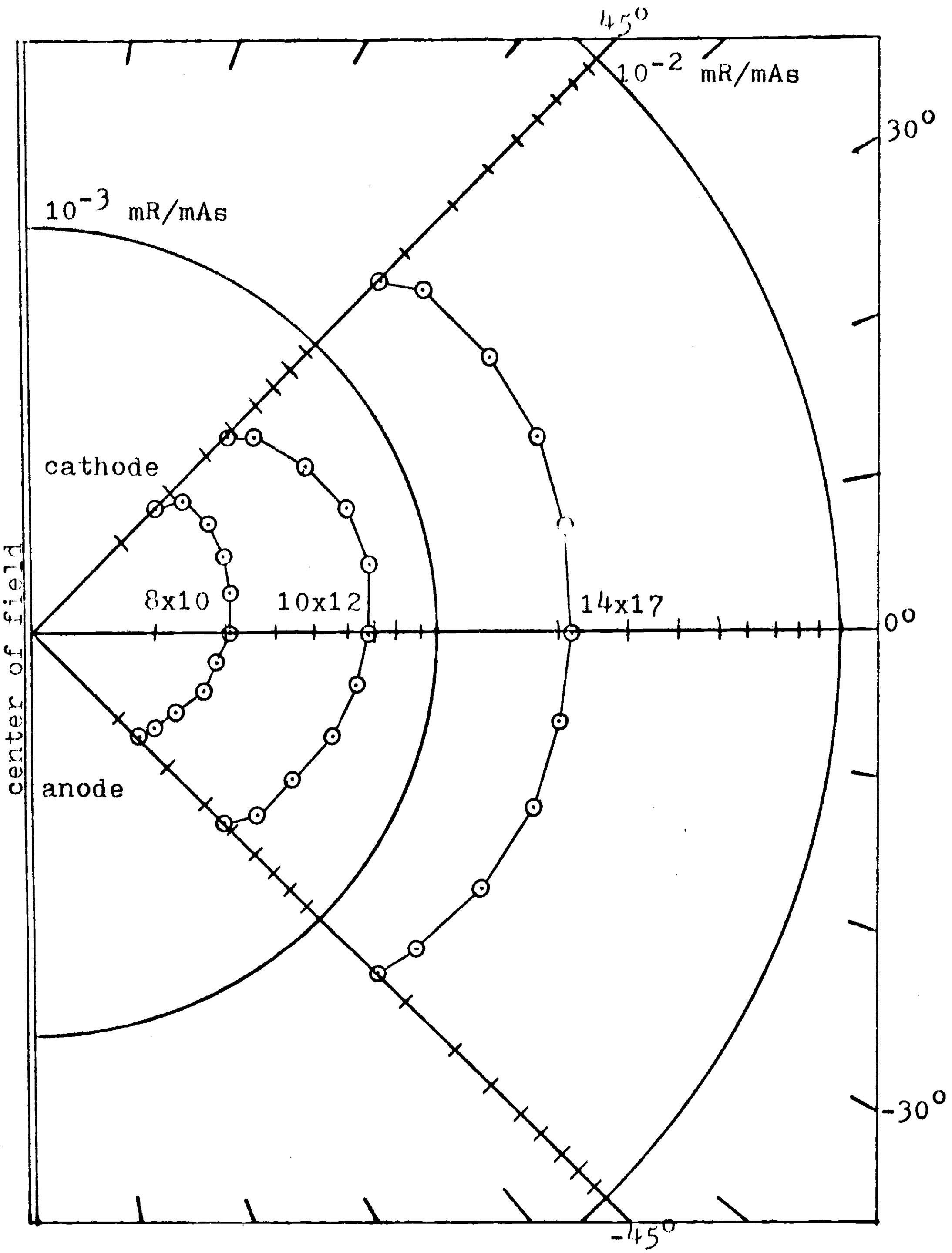

Figure 11. 90° Scatter Distribution at 40 kVp as a Function of Field Size. Expressed in mR/mAs at One Meter.

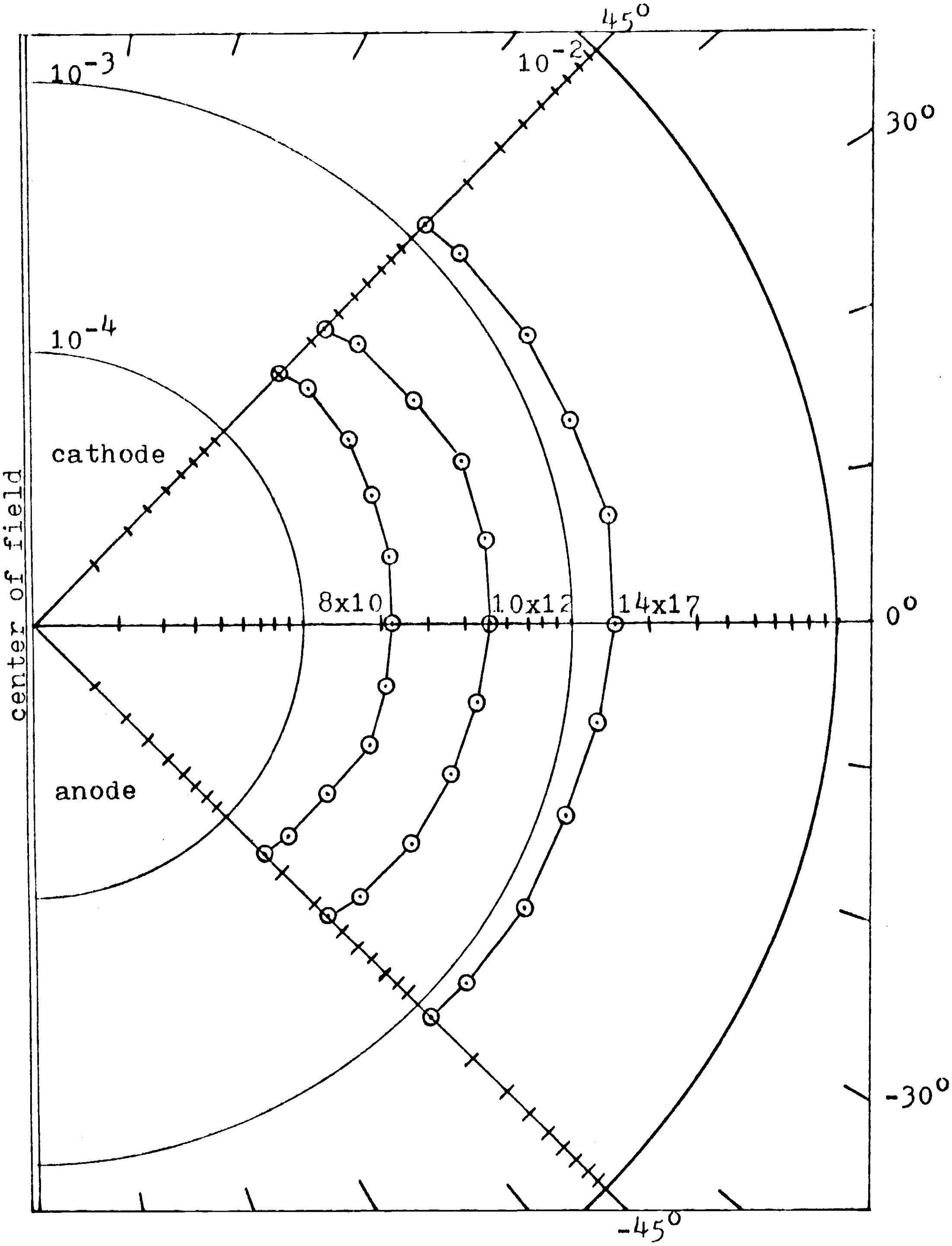

Figure 12. 90° Scatter Distribution at 40 kVp as a Function of Field Size. Expressed in Percentage of Useful Beam at One Meter.

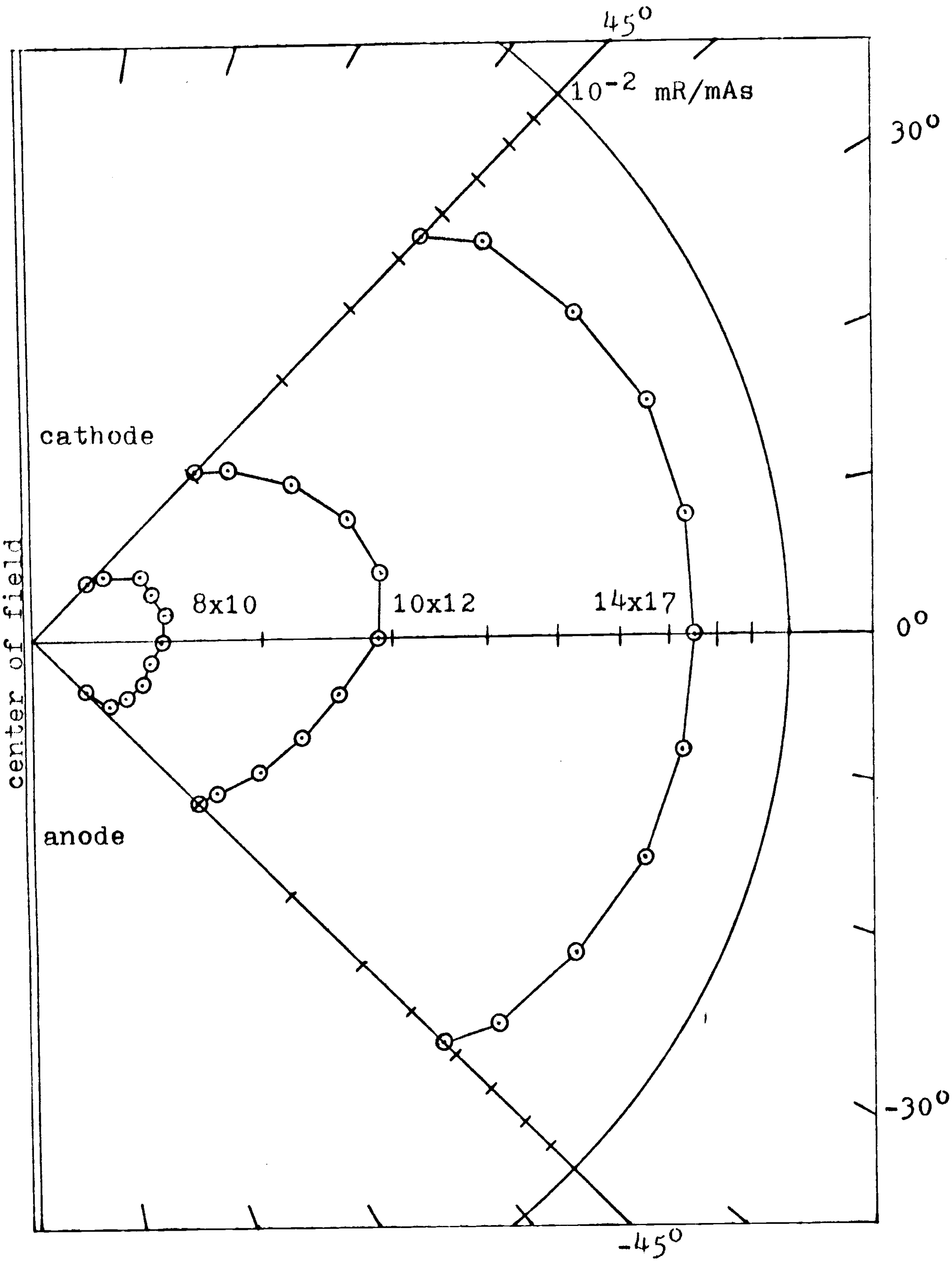

Figure 13. 90° Scatter Distribution at 60 kVp as a Function of Field Size. Expressed in mR/mAs at One Meter.

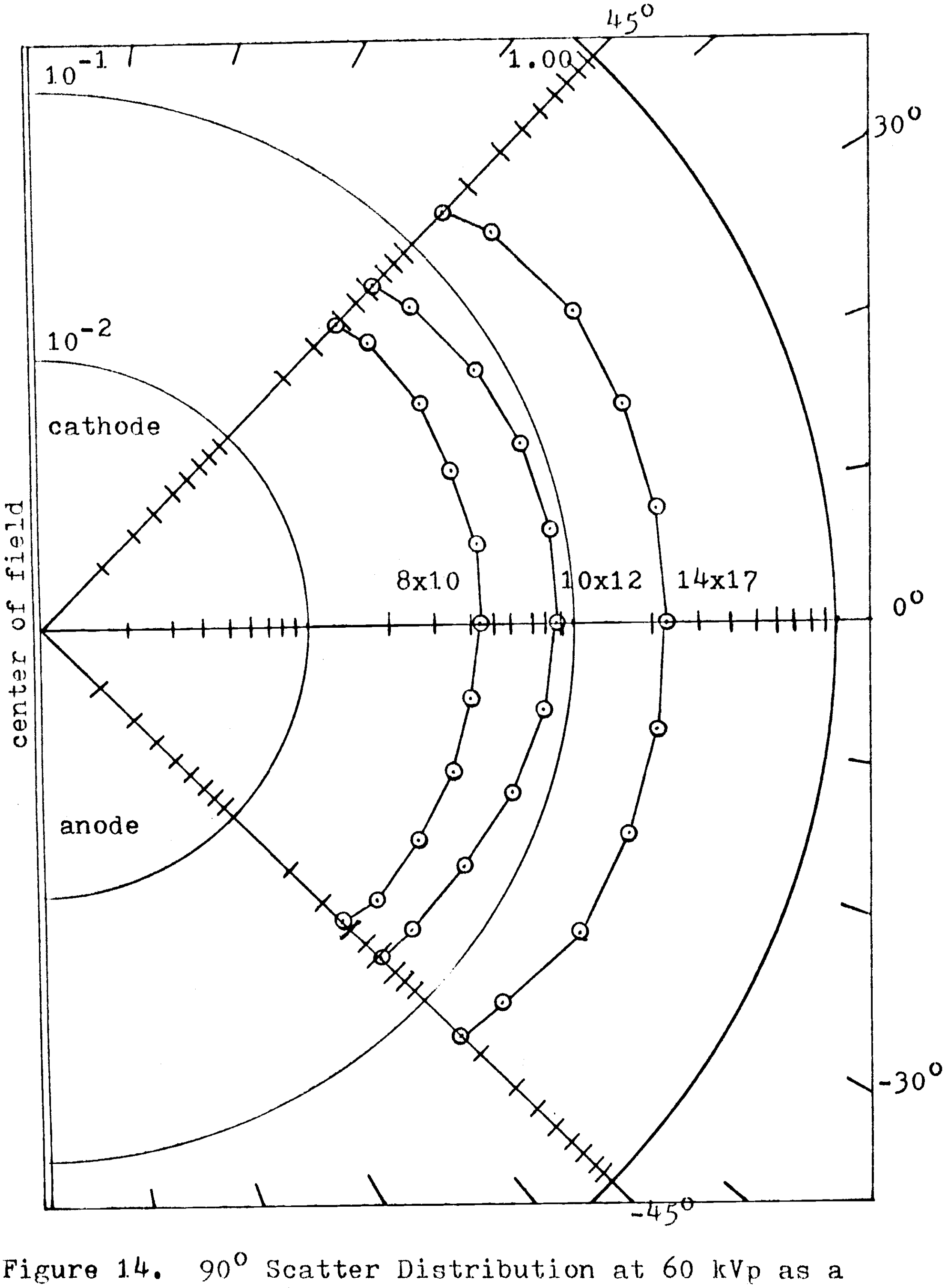

Figure 14. 90° Scatter Distribution at 60 kVp as a Function of Field Size. Expressed in Percentage of Useful Beam at One Meter.

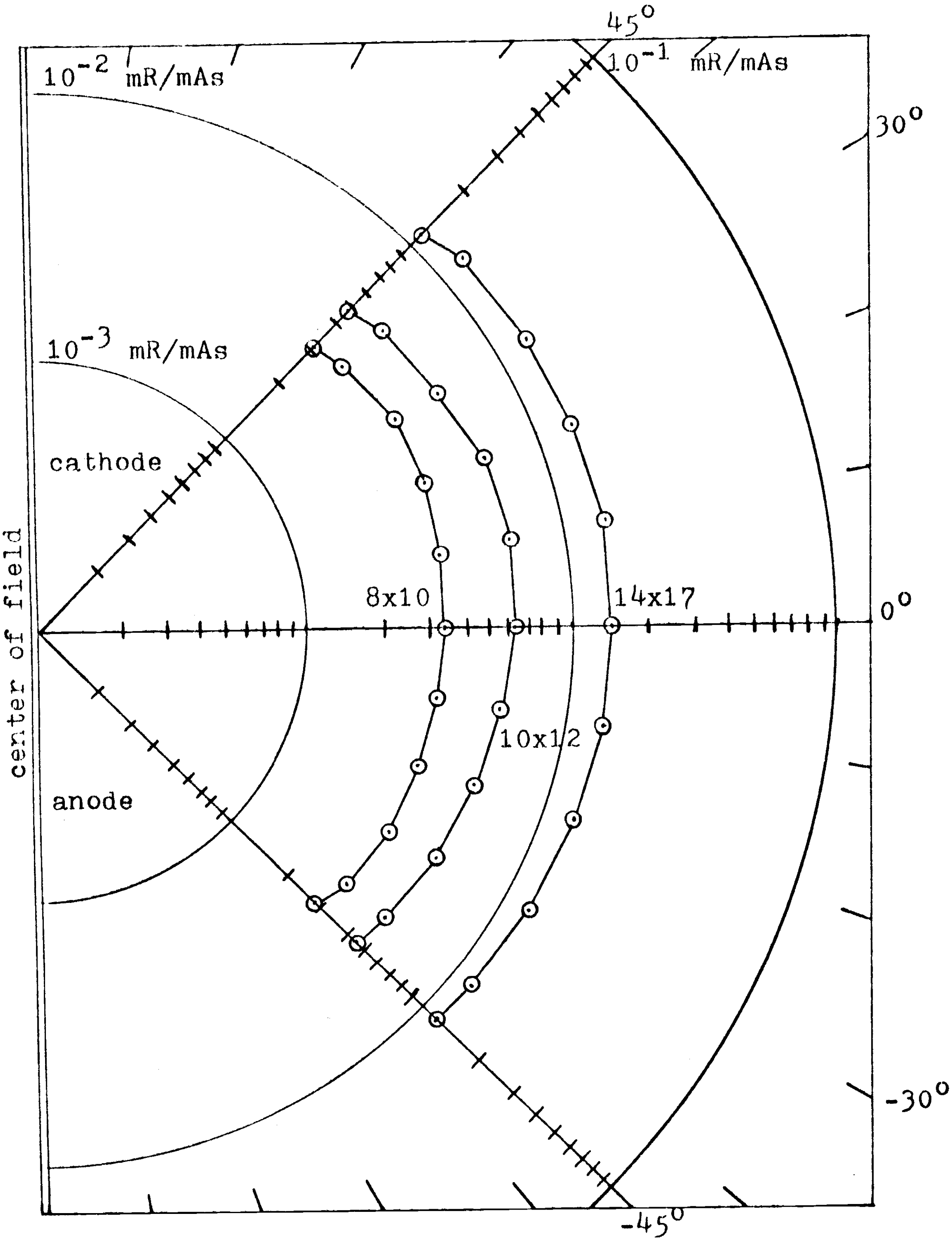

Figure 15. 90° Scatter Distribution at 80 kVp as a Function of Field Size. Expressed in mR/mAs at One Meter.

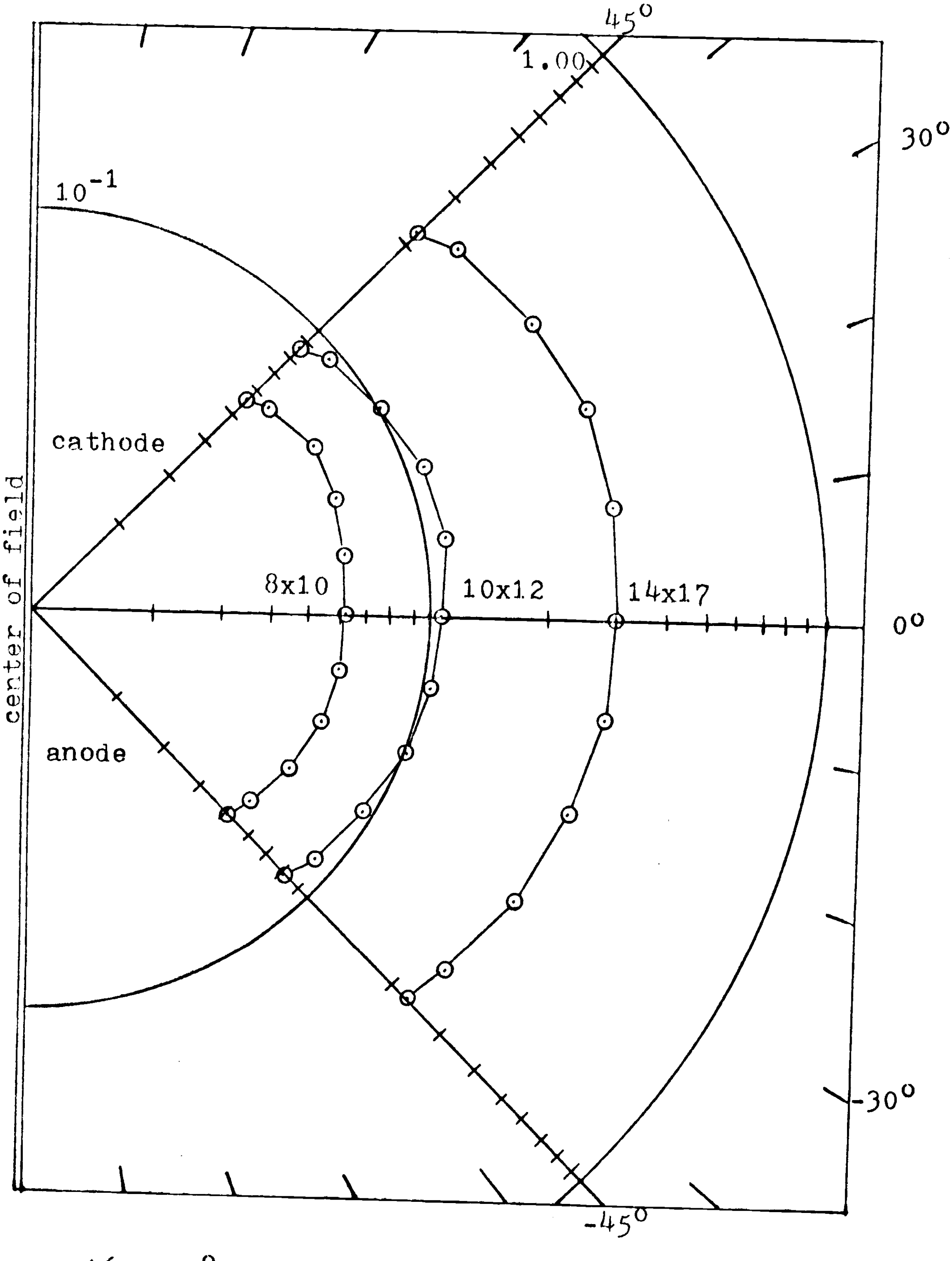

Figure 16. 90° Scatter Distribution at 80 kVp as a Function of Field Size. Expressed in Percentage of Useful Beam at One Meter.

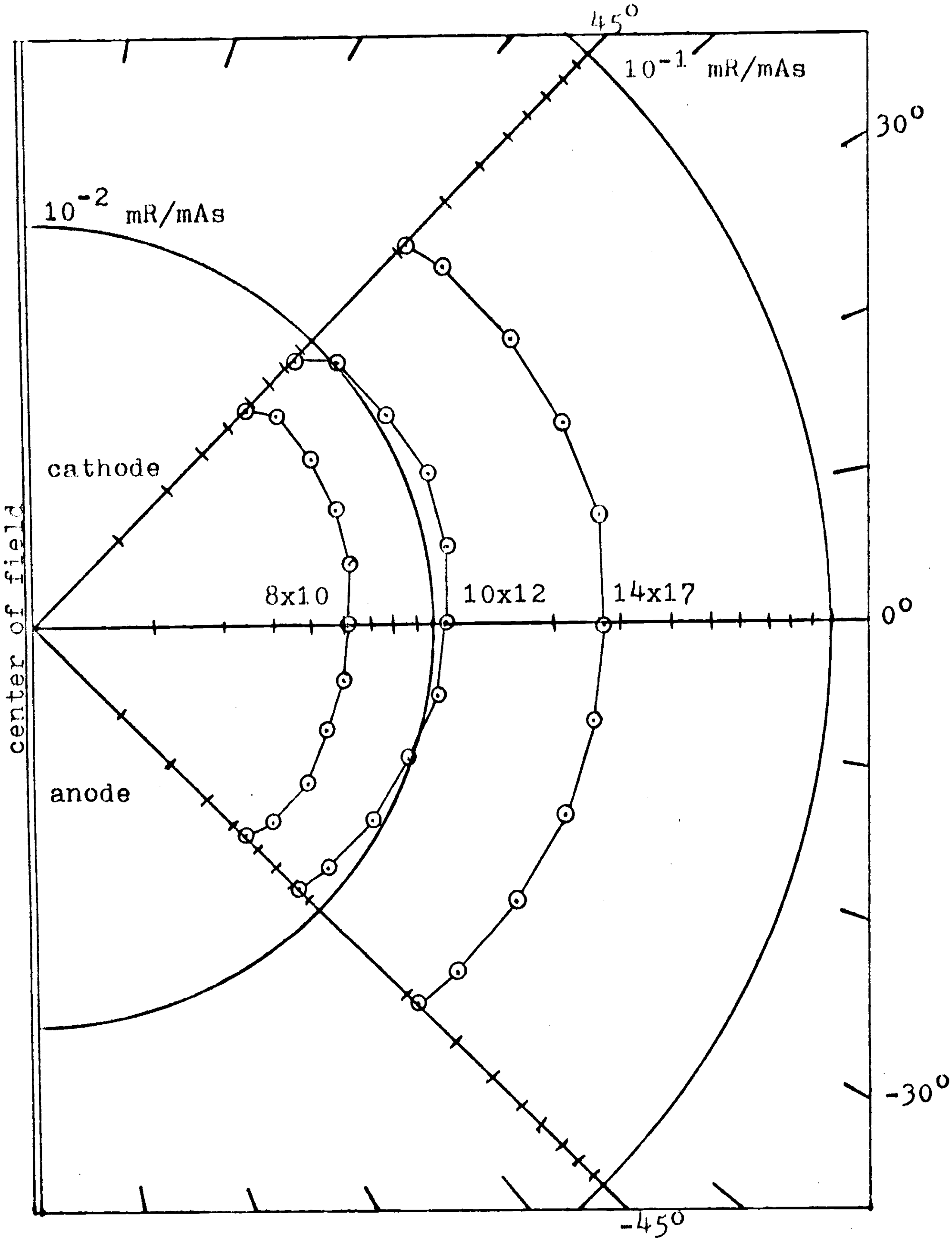

Figure 17. 90° Scatter Distribution at 100 kVp as a Function of Field Size. Expressed in mR/mAs at One Meter.

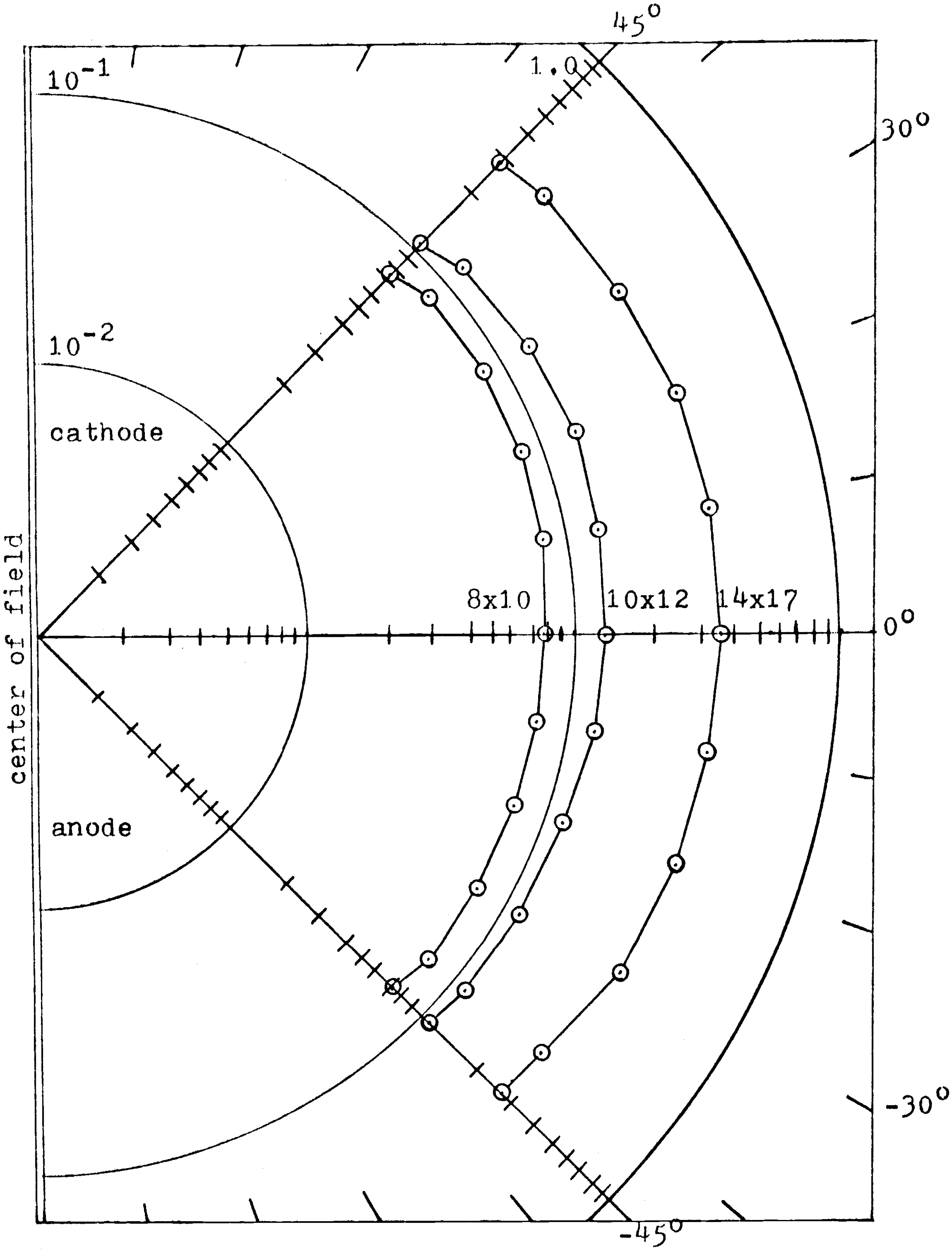

Figure 18. 90° Scatter Distribution at 100 kVp as a Function of Field Size. Expressed in Percentage of Useful Beam at One Meter.

V. DISCUSSION

It was found that the scattered radiation varies proportionally and independently with increasing voltage and with the field size at the film. This is in agreement with findings by Keane and Spiegler (27), Lorentzon (33), and Bomford and Burlin (4). They found that scatter increased as beam energy increased, and also as the field size was enlarged. At large values, however, the magnitude of the scatter tends to stabilize due to the cancelling effect of the greater thickness of medium from the center of the field (27,35,37,46).

Mahmoud and Vikterlof (34) found that for higher values of beam energy (200 kV therapy x rays), scatter isodose lines were virtually independent of field size. This was not demonstrated in this study, possibly due to the much lower range of beam energies used in diagnostic radiology.

The magnitude of the scattered radiation ranges from a minimum of 2.41×10^{-4} mR/mAs to a maximum of 2.89×10^{-2} mR/mAs through the parameters studied. The percentage of the useful beam ranged from 1.76×10^{-2} to 3.76×10^{-1}, which is in good agreement with values presented by Bomford and Burlin (4).

A significant variation of scatter occurs across the horizontal field for any given technic. There is a drop of 20% to 30% from the center field value to the 45^{o} value. This may be due to the field distribution and heel effect characteristic of the Mobile 100-15, since the maximum scatter occurs approximately 10^{o} to 20^{o} to the cathode side of the field, which would be expected if the field distribution were contributing an effect. Martin and Evans (35), and later Trout and Kelley (49) found that scatter exposure rate dropped sharply away from the edge of the beam. This may also be due to the increased thickness of absorber at the 45^{o} angle.

Leakage radiation represented less than 7% of the total radiation reaching the probe. In most cases is was very much less than this value. Table 1 gives the ratio of leakage to the total scatter exposure for each voltage and field size. The maximum allowable tube housing leakage from a diagnostic x-ray unit is 100 mR/h at one meter when the unit is being operated at its maximum continuous tube current at the maximum rated voltage (40). If the housing were to leak this amount in the geometry used for this study, 50 mR/h would reach the probe. If a linear relationship between tube current and exposure rate can be assumed, the net scatter at 100 kVp and 0.9 milliamperes (the maximum continuous tube current at 100 kVp for the Mobile 100-15) would be 93.6 mR/h. Therefore, the contribution from leakage to the total scatter at one meter would be 35% at 100 kVp.

In most cases, scattered radiation will present a greater potential hazard to adjacent personnel and the operator than tube housing leakage, as found in this study, and also by Martin and Evans (35). This appears to hold true for all cases except for very small field sizes (39,53).

In considering the source of scattered radiation, one must also consider the floor, walls, and nearby equipment. In situations where the attenuation of the primary beam is small, significant backscatter can be produced from the floor or wall in the direction of the beam. However, the primary attenuator, the patient, is generally considered to produce the majority of the scatter.

In dealing with any exposure situation, one must weigh benefit versus risk involved. The radiologic technologist must keep exposures to a minimum while still maintaining the necessary radiographic quality. Risk to the operator can be reduced by the use of protective clothing or shields, and to the patient by providing shielding for unexposed areas.

Another area of concern in the study of scatter, especially with mobile units, is the exposure delivered to persons not occupationally involved with radiation, such as other patients. The patient who cannot be moved to the x-ray department is given the examination in bed.

As was stated earlier, protection recommendations given by the advisory boards are a minimum of six feet of distance between personnel and the useful beam, and the use of protective shields or clothing by the operator. (40) It is of interest to determine the exposure theoretically delivered to a patient in an adjacent bed, and also to the operator, as a result of a mobile examination.

Exposure due to scatter for the technologist is dependent upon the workload of the unit used.[3] Exposures can be determined if the duration of the examination is known and the data for a typical scatter situation is available. For a nearby person, a one-time exposure from an examination would depend upon the technic. The typical hip examination of 80 kVp, one meter focus-film distance, requiring a 14 x 17-inch film, with an exposure of 50 mAs, would deliver an exposure of 0.21 mR to a person six feet away.

While the scatter values determined in this study are within limits set by current standards, it is still not known what effects even small exposures to radiation may have. Certainly it is advisable to review our laws and our standards with this in mind.

---

[3]Workload is defined as the product of the tube current in milliamperes and the total time of use of the unit in seconds or minutes per week. (40)

Table 1. Ratio of Tube Housing Leakage to Total Scatter Expressed in Percentage.

kVp	Ratio of Leakage to Scatter (Percent)		
	8 x 10	10 x 12	14 x 17
40	3.97	1.66	.529
60	.853	.439	.167
80	1.77	.987	.372
100	7.0	3.94	1.63

VI. SUMMARY

Scattering is a process which is present whenever radiation is used. By the use of proper shielding and protective coverings secondary exposures can be kept to a minimum.

Scatter varies proportionally with increasing voltage and increasing field size, and is the predominant factor in secondary radiation in diagnostic radiology. Tube housing leakage is small in proportion except when very small field sizes are used.

The results of this study indicate that exposures to personnel are within presently acceptable limits. Radiation exposures should be kept to a minimum using the present standards for equipment use, since it is still not known what effect even small exposures to radiation may have on the human system. Therefore, it would be prudent to examine our radiation protection standards and recommendations with the thought to create a safer radiation situation.

BIBLIOGRAPHY

1. Andrews, Howard L. A nomogram for calculating the energy relations in Compton scattering. Health Physics 18: 158-159. 1970.

2. Batho, Harold F. X-ray protection. Journal of the Canadian Association of Radiologisys 1:48-51. 1950.

3. Bewley, D. K. An integrating machine for estimating the dosage rate of scattered x rays. British Journal of Radiology 24:213-214. 1951.

4. Bomford, C. K. and T. E. Burlin. The angular distribution of radiation scattered from a phantom exposed to 100-300 kVo x rays. British Journal of Radiology 36: 436-439. 1963.

5. Brown, J. G. Observations of the scattered radiation inside and outside a 1,000-Curie cobalt^{60} teletherapy room. Radiology 61:82-87. 1953.

6. Bruce, W. R. and H. E. Johns. Monte Carlo calculations on the spectrum of scattered radiation produced in water by x-ray beams of interest in radiotherapy. Radiology 68:100-101. 1957.

7. Burr, R. C. and A. F. Holloway. Radiation hazards and protection in diagnostic radiology. Journal of the Canadian Association of Radiologists 11:75-80. 1960.

8. Cederlund, J., K. Liden and M. Lindgren. Distribution of scattered radiation in a fluoroscopic room. Acta Radiologica 44:457-466. 1955.

9. Cormack, D. V. A comparison of theoretical and experimental spectral distributions of scattered x-rays. Journal of the Canadian Association of Radiologists 11: 40-43. 1960.

10. Cormack, D. V. and D. G. Burke. Spectral distributions of primary and scattered 140 kvp x-rays. Radiology 74: 743-752. 1960.

11. Cormack, D. V. and H. E. Johns. Spectral distribution of scattered radiation from a cobalt 60 unit. British Journal of Radiology 31:497-502. 1958.

12. Cormack, D. V. and S. Mak. Spectra of scattered radiation at points off the beam axis. Radiology 72:107. 1959.

13. Cowing, Russell F. and Charles K. Spalding. A survey of scattered radiation from fluoroscopic units in fifteen institutions. Radiology 53:569-574. 1949.

14. Flatby, Jon and Sem Maudal. Some measurements of scattered radiation from Roentgen diagnostic beams. Acta Radiologica 46:690-699. 1956.

15. General Electric Company Technical Service. How to prepare an x-ray technic chart. No publisher listed, 1964. 16 p. (Publication no. 13A-3478F.)

16. Glasser, O., et al. Physical foundations of radiology. 3d ed. New York, Harper and Row, 1965. 503 p.

17. Greening, J. R. A method of determining the wavelength distribution of the x-radiation at a point in a scattering medium. British Journal of Radiology 24: 204-206. 1951.

18. Greening, J. R. and C. W. Wilson. The wavelength of the x radiation at a depth in water irradiatied by beams of x rays. British Journal of Radiology 24:605-612. 1951.

19. Hemphill, Fay M., Frances B. Locke and Rudolph D. Hesselgren. Diagnostic radiation utilization in selected short-term general hospitals. Rockville, United States Public Health Service, 1970. 52 p. (Publication no. BRH/DBE 70-8.)

20. Hendee, W. R. and J. L. Ellis. Scattering of gamma radiation from semi-infinite slabs. Health Physics 12: 673-681. 1966.

21. Herbert, Donald. Dependence of exposure rate upon field size and shape. British Journal of Radiology 44: 75. 1971.

22. Hettinger, Gunnar. Angular and spectral distributions of backscatter radiation from slabs of water, brass, and lead irradiated by photons between 50 and 250 keV. Acta Radiologica 54:129-152. 1960.

23. Hettinger, Gunnar and Kurt Liden. Scattered radiation in a water phantom irradiated by Roentgen photons between 50 and 250 keV. Acta Radiologica 53:73-92. 1960.

24. International Commission on Radiation Units and Measurements. Radiation quantities and units. Washington, D. C., 1968. 8 p. (Report no. 11.)

25. Johns, Harold Elford and John Robert Cunningham. The physics of radiology. 3d ed. Springfield, Charles C. Thomas, 1969. 800 p.

26. Johns, H. E. and E. K. Darby. The distribution of radiation near the geometrical edge of an x-ray beam. British Journal of Radiology 23:193-197. 1950.

27. Keane, B. E. and G. Spiegler. Stray radiation from diagnostic x-ray beams. British Journal of Radiology 24:198-203. 1951.

28. Kelley, John P. Personal communication. 1971.

29. Lamerton, L. F. and Margaret Winsborough. An approach to the problem of scattering of high voltage radiation in non-homogeneous and limited media. British Journal of Radiology 23:236-244. 1950.

30. Landauer, R. S. The use of dental films in the determination of stray radiation. Radiology 8:512-517. 1927.

31. Leucutia, T. Unexpected sources of stray Roentgen radiation. American Journal of Roentgenology, Radium Therapy and Nuclear Medicine 67:647-650. 1952.

32. Lindell, Bo. Secondary Roentgen radiation. Acta Radiologica 41:353-376. 1954.

33. Lorentzon, Lars. Secondary Roentgen radiation from was, Al, Fe, and Pb at tube voltages between 40 and 170 kV. Acta Radiologica 41:201-208. 1954.

34. Mahmoud, K. A. and K. J. Vikterlof. Scattered radiation in a rotation therapy room using 200 kV Roentgen rays. Acta Radiologica 47:407-415. 1957.

35. Martin, J. H. and Ann Evans. Radiation outside the defined field. British Journal of Radiology 32:7-12. 1959.

36. Martin, J. H. and Gwenda M. Muller. Quantity and quality of scattered x rays. British Journal of Radiology 34:227-235. 1961.

37. Mattson, Ove. Some studies on primary and secondary radiation and on secondary screening in diagnostics up to 200 kV. Acta Radiologica 46:621-631. 1956.

38. McEwan, A. C. An approximation for estimating Compton scatter from a cuboid phantom. Physics in Medicine and Biology 14:627-630. 1969.

39. McEwan, A. C. The relative importance of leakage and scatter in megavoltage installation design. Physics in Medicine and Biology 14:659-660. 1969.

40. National Council on Radiation Protection and Measurements. Medical x-ray and gamma-ray protection for energies up to 10 MeV. Equipment design and use. Washington, D. C., 1968. 66 p. (Report no. 33.)

41. National Council on Radiation Protection and Measurements. Medical x-ray and gamma-ray protection for energies up to 10 MeV. Structural shielding design and evaluation. Washington, D. C., 1970. 117 p. (Report no. 34.)

42. National Council on Radiation Protection and Measurements. Basic radiation protection criteria. Washington, D. C., 1971. 135 p. (Report no.39.)

43. O'Connor, J. E. The variation of scattered x-rays with density in an irradiated body. Physics in Medicine and Biology 1:352-369. 1957.

44. Oregon State Board of Health. Regulations for control of radiation for use in the healing arts. Rev. ed. No publisher listed, 1969. 37 p.

45. Reiss, K. H. Scattered radiation and characteristic film curve. Radiology 80:663-667. 1963.

46. Sanders, Aaron P., et al. Right-angle scatter for x-ray beams of 0.14 mm. to 2.5 mm. copper h. v. l. Radiology 75:595-598. 1960.

47. Spalding, Charles K. and Russell F. Cowing. A survey of exposures received by hospitalized patients during routine diagnostic x-ray procedures. Radiology 82: 113-119. 1964.

48. Spiegler, G. and B. E. Keane. Scatter doses received on the lower extremities of the diagnostic radiologist. British Journal of Radiology 28:140-146. 1955.

49. Trout, E. Dale and John P. Kelley. Scattered radiation in a phantom from a diagnostic quality radiation. Radiology 85:546-554. 1965.

50. Victoreen Instrument Division. Radiation standardization. Medical dosimetry. Cleveland, 1969. (Brochure no. 3195A.)

51. Walstam, Rune. Dose measurements on secondary Roentgen radiation. Acta Radiologica 41:348-352. 1954.

52. Wilsey, R. B., D. H. Strangways and G. M. Corney. Experiments in the photographic monitoring of stray x-rays. Part I. General considerations. The choice of film-calibrating radiations in Roentgen therapy at 220 kvp and 1,000 kvp. Radiology 66:408-417. 1956.

53. Wilsey, R. B., H. R. Splettstosser and D. H. Strangways. Experiments in the photographic monitoring of stray x-rays. Part II. The characteristics of the stray radiations, and the choice of film-calibrating radiations in diagnostic radiology. Radiology 66:418-428. 1956.

54. Winkler, Norlin T. Minimizing radiation exposure of patients and personnel. Radiologic Technology 41: 142-149. 1969.

APPENDICES

APPENDIX A

Scatter Data

Table 2. 90^{o} Scatter Distribution at One Meter from an 8 x 10-inch Field at 40 kVp.

Horizontal Angle	Scatter	
	mR/mAs	Percent Useful Beam
0^{o}	3.155×10^{-4}	2.3×10^{-2}
10^{o}	3.18	2.32
20^{o}	3.22	2.36
30^{o}	3.25	2.38
40^{o}	3.08	2.25
45^{o}	2.74	2.0
-10^{o}	2.96	2.16
-20^{o}	2.86	2.15
-30^{o}	2.64	1.93
-40^{o}	2.50	1.82
-45^{o}	2.41	1.76

Table 3. 90° Scatter Distribution at One Meter from an 8 x 10-inch Field at 60 kVp.

Horizontal Angle	Scatter	
	mR/mAs	Percent Useful Beam
0°	1.48×10^{-3}	4.47×10^{-2}
10°	1.54	4.67
20°	1.475	4.46
30°	1.485	4.48
40°	1.35	4.09
45°	1.285	3.80
-10°	1.38	4.18
-20°	1.395	4.23
-30°	1.33	4.03
-40°	1.325	4.01
-45°	1.235	3.74

Table 4. 90° Scatter Distribution at One Meter from an 8 x 10-inch Field at 80 kVp.

Horizontal Angle	Scatter	
	mR/mAs	Percent Useful Beam
0°	3.46×10^{-3}	6.29×10^{-2}
10°	3.55	6.47
20°	3.72	6.78
30°	3.74	6.80
40°	3.31	6.03
45°	3.10	5.65
-10°	3.44	6.26
-20°	3.37	6.12
-30°	3.24	5.89
-40°	3.07	5.58
-45°	2.89	5.25

Table 5. 90^{o} Scatter Distribution at One Meter from an 8 x 10-inch Field at 100 kVp.

Horizontal Angle	Scatter	
	mR/mAs	Percent Useful Beam
0^{o}	6.09×10^{-3}	7.92×10^{-2}
10^{o}	6.42	8.35
20^{o}	6.55	8.55
30^{o}	6.65	8.65
40^{o}	6.42	8.35
45^{o}	5.87	7.62
-10^{o}	6.03	7.84
-20^{o}	5.98	7.79
-30^{o}	6.02	7.82
-40^{o}	5.91	7.70
-45^{o}	5.43	7.07

Table 6. 90^{o} Scatter Distribution at One Meter from a 10 x 12-inch Field at 40 kVp.

Horizontal Angle	Scatter	
	mR/mAs	Percent Useful Beam
0^{o}	6.95×10^{-4}	5.06×10^{-2}
10^{o}	7.10	5.19
20^{o}	6.91	5.05
30^{o}	6.03	4.39
40^{o}	5.38	3.93
45^{o}	4.82	3.52
-10^{o}	6.59	4.80
-20^{o}	6.12	4.46
-30^{o}	5.59	4.07
-40^{o}	5.25	3.83
-45^{o}	4.75	3.47

Table 7. 90^{o} Scatter Distribution at One Meter from a 10 x 12-inch Field at 60 kVp.

Horizontal Angle	Scatter	
	mR/mAs	Percent Useful Beam
0^{o}	2.88×10^{-3}	8.70×10^{-2}
10^{o}	2.96	8.96
20^{o}	2.82	8.55
30^{o}	2.63	7.95
40^{o}	2.29	6.90
45^{o}	2.055	6.22
-10^{o}	2.69	8.05
-20^{o}	2.48	7.50
-30^{o}	2.24	6.79
-40^{o}	2.06	6.24
-45^{o}	2.00	6.06

Table 8. 90° Scatter Distribution at One Meter from a 10 x 12-inch Field at 80 kVp.

Horizontal Angle	Scatter	
	mR/mAs	Percent Useful Beam
0°	6.27×10^{-3}	11.4×10^{-2}
10°	6.60	12.0
20°	6.52	11.85
30°	5.87	10.68
40°	5.23	9.50
45°	4.78	8.70
-10°	5.97	10.85
-20°	5.69	10.12
-30°	5.17	9.40
-40°	4.89	8.90
-45°	4.57	8.32

Table 9. 90^{o} Scatter Distribution at One Meter from a 10 x 12-inch Field at 100 kVp.

Horizontal Angle	Scatter	
	mR/mAs	Percent Useful Beam
0^{o}	11.15×10^{-3}	14.5×10^{-2}
10^{o}	11.92	15.0
20^{o}	11.95	15.55
30^{o}	11.0	14.3
40^{o}	10.05	13.08
45^{o}	8.53	11.10
-10^{o}	10.77	14.0
-20^{o}	9.78	12.72
-30^{o}	9.27	12.07
-40^{o}	8.72	11.35
-45^{o}	8.33	10.83

Table 10. 90^{o} Scatter Distribution at One Meter from a 14 x 17-inch Field at 40 kVp.

Horizontal Angle	Scatter	
	mR/mAs	Percent Useful Beam
0^{o}	2.215×10^{-3}	16.15×10^{-2}
10^{o}	2.30	16.75
20^{o}	2.19	15.95
30^{o}	2.02	14.75
40^{o}	1.865	13.6
45^{o}	1.717	12.5
-10^{o}	2.145	15.7
-20^{o}	2.078	15.15
-30^{o}	1.922	14.0
-40^{o}	1.745	12.75
-45^{o}	1.645	12.0

Table 11. 90^{o} Scatter Distribution at One Meter from a 14 x 17-inch Field at 60 kVp.

Horizontal Angle	Scatter	
	mR/mAs	Percent Useful Beam
0^{o}	7.6×10^{-3}	23.0×10^{-2}
10^{o}	7.7	23.3
20^{o}	7.54	22.8
30^{o}	6.93	21.0
40^{o}	6.20	18.8
45^{o}	5.50	16.65
-10^{o}	7.43	22.45
-20^{o}	7.21	21.8
-30^{o}	6.80	20.58
-40^{o}	6.15	18.6
-45^{o}	5.72	17.25

Table 12. 90° Scatter Distribution at One Meter from a 14 x 17-inch Field at 80 kVp.

Horizontal Angle	Scatter	
	mR/mAs	Percent Useful Beam
0°	16.70×10^{-3}	30.4×10^{-2}
10°	17.0	31.0
20°	16.68	30.38
30°	15.38	28.0
40°	14.35	26.2
45°	12.88	23.4
-10°	16.42	29.9
-20°	15.45	28.1
-30°	14.85	27.0
-40°	13.55	24.6
-45°	12.85	23.3

Table 13. 90° Scatter Distribution at One Meter from a 14 x 17-inch Field at 100 kVp.

Horizontal Angle	Scatter	
	mR/mAs	Percent Useful Beam
0°	27.65×10^{-3}	36.0×10^{-2}
10°	28.90	37.6
20°	27.95	36.4
30°	25.65	33.4
40°	23.95	30.8
45°	22.20	28.9
-10°	27.10	35.2
-20°	26.20	34.0
-30°	24.70	32.2
-40°	22.85	29.7
-45°	21.65	28.2

APPENDIX B

Miscellaneous

Table 14. Beam Quality Factors. General Electric Mobile 100-15. Collimator Removed.

	Kilovolts Peak			
	40	60	80	100
Useful Beam Exposure Rate R/min	.822	1.98	3.297	4.605
First H. V. L. mm. Al	1.15	1.60	2.20	2.85
Second H. V. L. mm. Al	1.75	2.40	3.30	4.05
Inherent Filtration mm. Al	2.00	2.00	2.22	2.50
Effective Energy keV	22.5	25	28	31
Homogeneity Coefficient	.657	.667	.667	.695

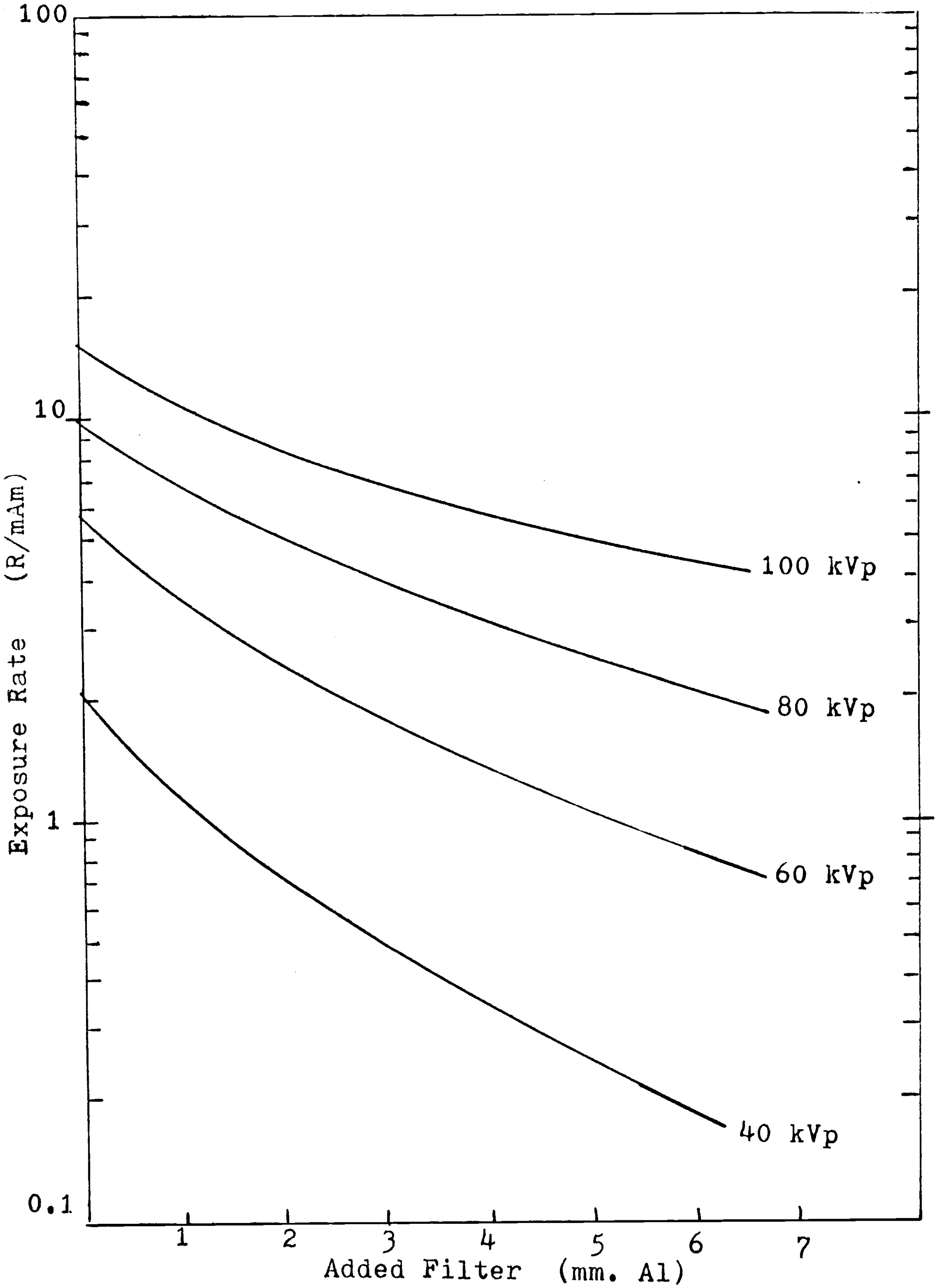

Figure 19. Attenuation Curves in Aluminum for the General Electric Mobile 100-15 X-ray Unit.

Table 15. Time Response Correction Factors for the Victoreen 555 Radocon with 0.1DA Probe.

Rate Scale	Correction Factor Krc
3 mR/min	1.152
10 mR/min	1.137
30 mR/min	1.09
100 mR/min	1.02
300 mR/min	1.00
1 R/min	1.00
3 R/min	1.00
10 R/min	1.00

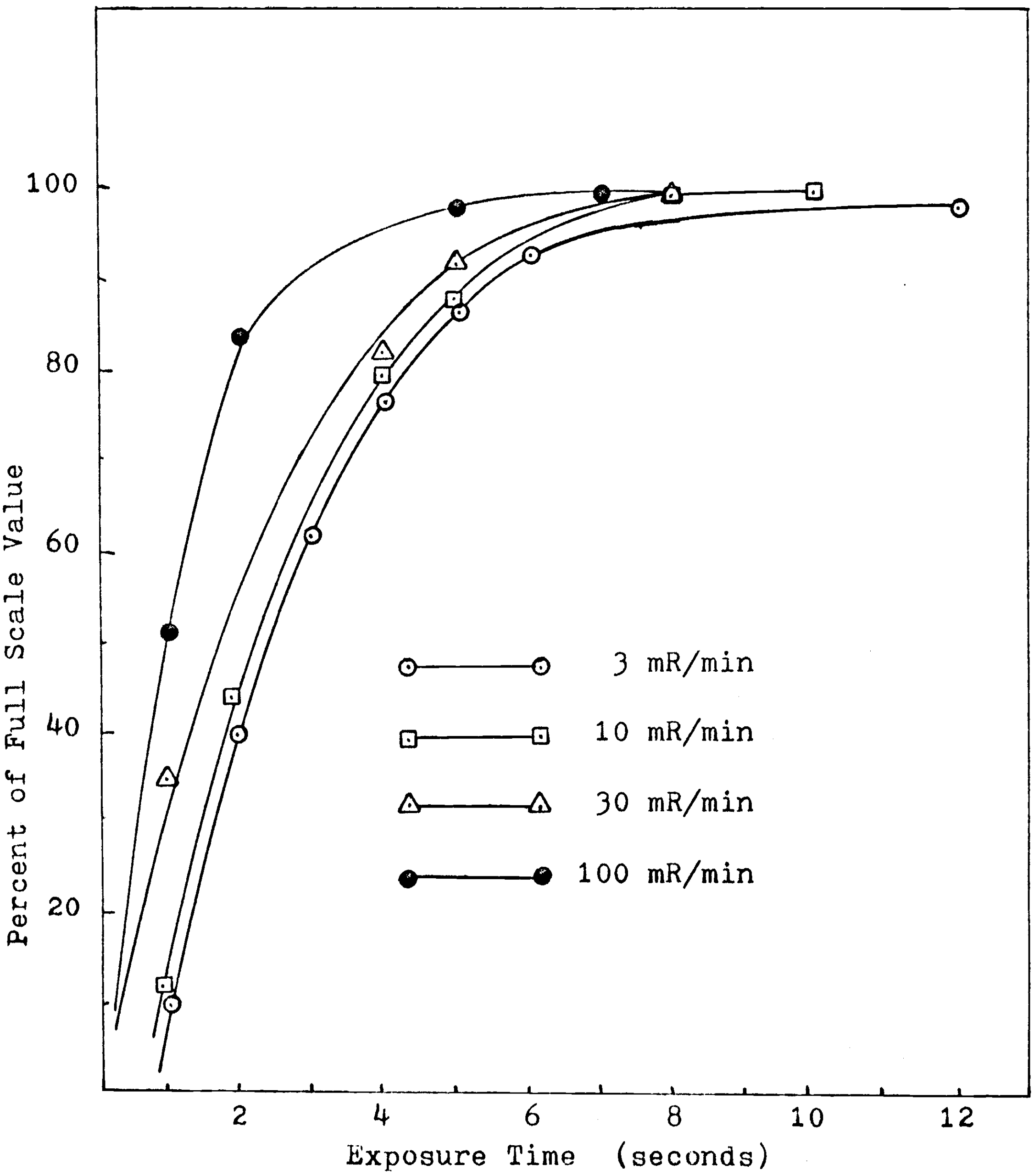

Figure 20. Time Response of the Victoreen 555 Radocon with 0.1DA Probe.

Table 16. Energy Response Correction Factors for the Victoreen 555 Radocon with 0.1DA Probe.

Kilovolts Peak	Correction Factor Kr
40	1.067
60	1.062
80	1.06
100	1.058

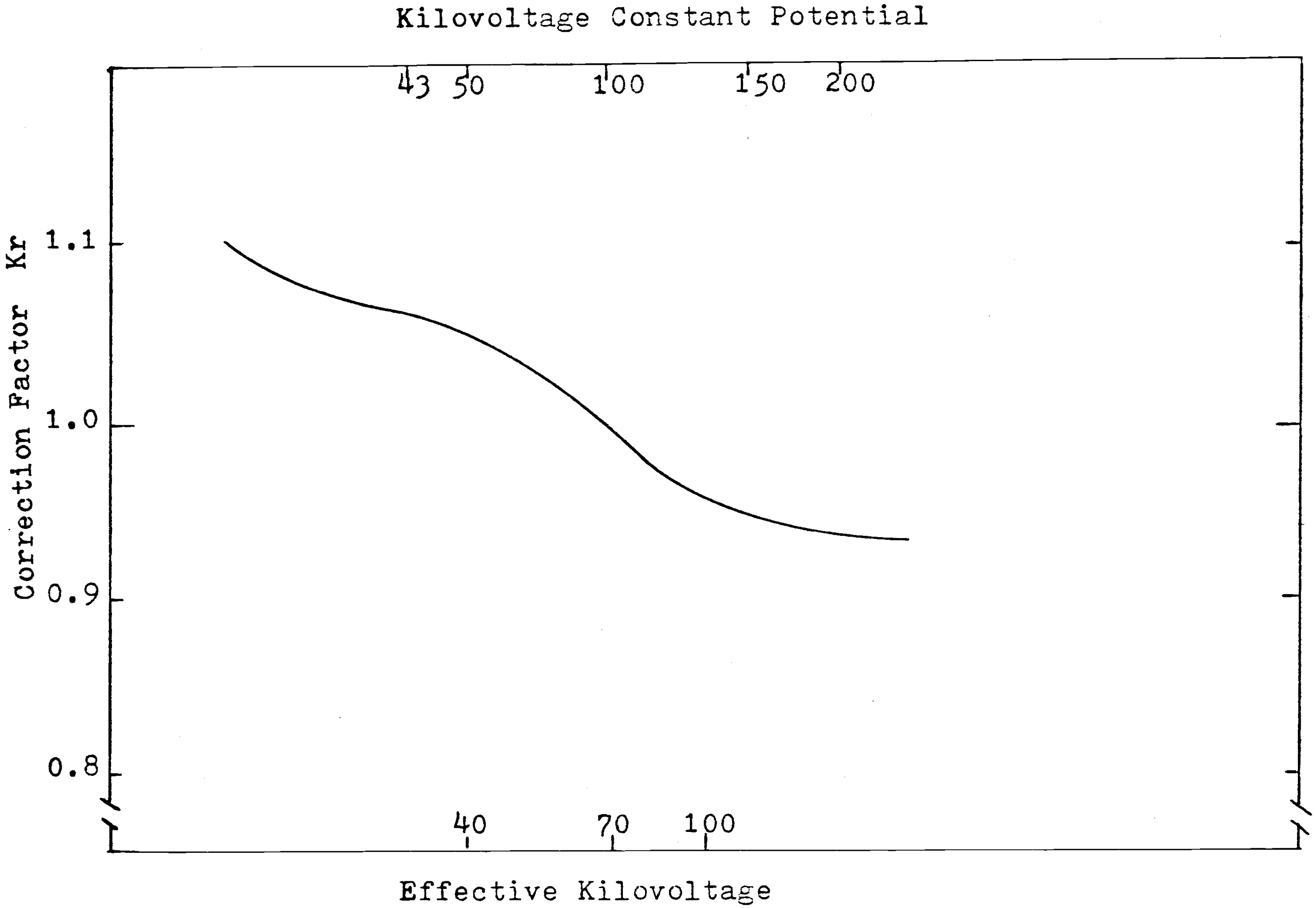

Figure 21. Energy Response of the Victoreen 555 Radocon and 0.1DA Probe. Correction Factors.

Table 17. Horizontal Distribution of X-ray Tube Housing Leakage. General Electric Mobile 100-15. Beam Blocked at Beam Port.

Horizontal Angle	Leakage Radiation (mR/mAs)			
	40 kVp	60 kVp	80 kVp	100 kVp
	$\times 10^{-6}$	$\times 10^{-6}$	$\times 10^{-5}$	$\times 10^{-4}$
0°	11.75	10.86	6.24	4.57
10°	10.5	12.7	4.81	4.35
20°	9.28	10.05	4.38	3.64
30°	<8.34	<9.72	3.74	2.03
40°	<8.34	<9.72	2.68	1.632
45°	<8.34	<9.72	2.14	1.497
-10°	9.28	10.13	4.99	4.35
-20°	<8.34	10.86	4.46	4.08
-30°	<8.34	<9.72	3.80	3.71
-40°	<8.34	<9.72	2.67	2.82
-45°	<8.34	<9.72	2.14	2.56

Table 18. Equipment Model and Serial Numbers.

X-ray Unit:

General Electric Mobile 100-15

Model no. 11CE8A-3

Serial no. 723793

Head: General Electric

Model no. 11AA5A2

Serial no. 724185

Mascot Collimator: Videx Corporation

Model no. FF50

Instruments:

Victoreen Radocon

Model no. 555

Serial no. 123

555-10LA Probe

Serial no. 102

555-0.1DA Probe

Serial no. 105
